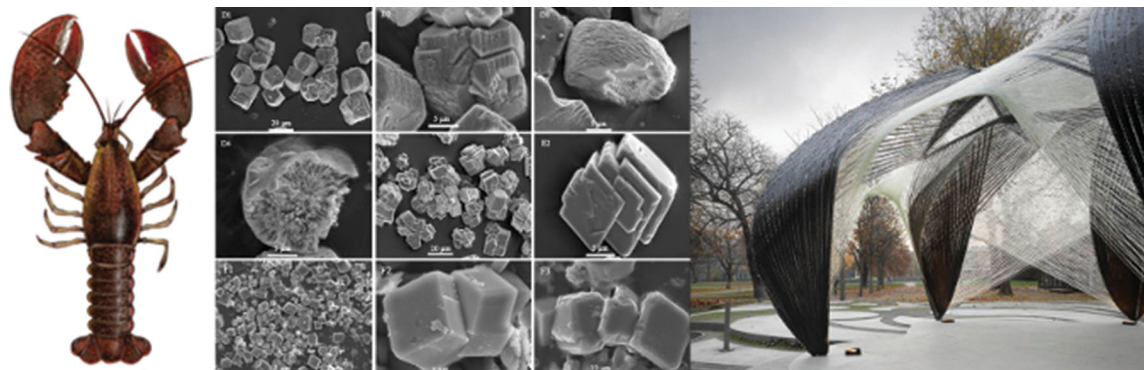


Crustacean-Derived Biomimetic Components and Nanostructured Composites

Lessa Kay Grunenfelder, Steven Herrera, and David Kisailus*



From the Contents

1. Introduction	3208
2. Cuticle Structure	3209
3. Specific Examples of Crustaceans	3210
4. Biomimetic Composites Inspired by the Crustacean Cuticle	3218

Over millions of years, the crustacean exoskeleton has evolved into a rigid, tough, and complex cuticle that is used for structural support, mobility, protection of vital organs, and defense against predation. The crustacean cuticle is characterized by a hierarchically arranged chitin fiber scaffold, mineralized predominately by calcium carbonate and/or calcium phosphate. The structural organization of the mineral and organic within the cuticle occurs over multiple length scales, resulting in a strong and tough biological composite. Here, the ultrastructural details observed in three species of crustacean are reviewed: the American lobster (*Homarus americanus*), the edible crab (*Cancer pagurus*), and the peacock mantis shrimp (*Odontodactylus scyllarus*). The Review concludes with a discussion of recent advances in the development of biomimetics with controlled organic scaffolding, mineralization, and the construction of nanoscale composites, inspired by the organization and formation of the crustacean cuticle.

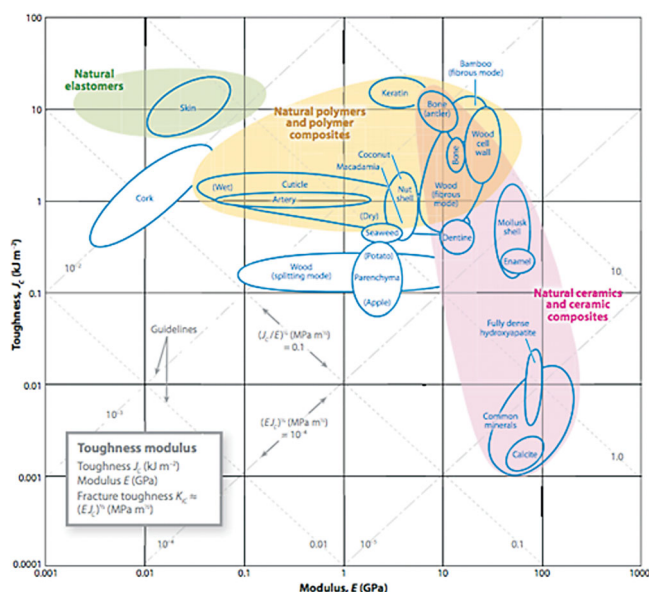


Figure 1. Ashby plot of toughness and modulus for natural materials (cuticle displayed with “natural polymers and polymer composites”). Reproduced with permission.^[6] Copyright 2010, Annual Reviews.

1. Introduction

Nature has evolved strategies to synthesize mechanically robust materials. These biological composites are formed from biopolymers and minerals, and achieve high strength, stiffness, and toughness, despite benign processing conditions and a limited selection of constituent materials.^[1] The properties observed in biomineralized materials stem from their hierarchical structure, along with the degree, type, and controlled location of mineral content.^[2–4] Biological systems demonstrate the ability to control size, crystallinity, morphology, phase and orientation of mineral during growth.^[5] The controlled nano- and microstructural features present in biological samples lead to material properties that exceed those of the constituent material components.^[1,2,4,6] Additionally, the hierarchical structure of biocomposites results in multifunctionality at different structural levels and over multiple length scales.^[6] Through optimized synthesis methods and smart material design, natural composites display high stiffness and toughness (Figure 1). As has been the case throughout history, scientists are learning from their surroundings, and drawing inspiration from nature to develop novel synthetic materials. This field of study is known as biomimetics. A topic search of “biomimetic” on the Web of Science shows the increasing interest in this topic area in recent years (Figure 2). One natural structure that has achieved considerable attention in the field of biomimetics is the arthropod exoskeleton.

The phylum Arthropoda is the largest and most diverse in the animal kingdom.^[7] Arthropods arose primarily during the so-called Cambrian explosion (550–600 million years ago),^[8,9] owing in part to increased levels of calcium ions in seawater which made possible the development of mineralized hard bodies.^[7,10] Arthropods are a varied collection of animals,

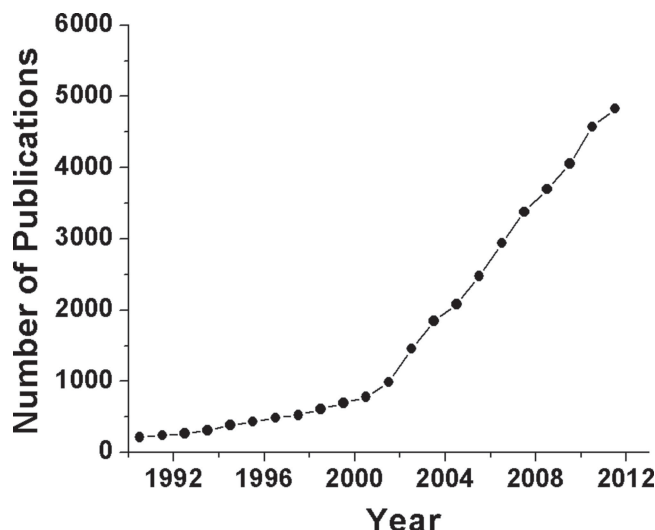


Figure 2. Topic search of “biomimetic” on the Web of Science, results by year.

adapted to survival in almost any habitat, spanning land, sea, fresh water, and air.^[8,11,12]

The unifying feature among arthropods is their tough and damage resistant exoskeleton. This exoskeleton, or cuticle, has been optimized to serve multiple functions, including support, protection against predation, prevention of swelling, and as a barrier to desiccation.^[8,13] In the Arthropod family, members of the subphylum Crustacea exhibit some of the most complex body plans, with wide ranging morphologies in their thoracic and abdominal segments, as well as their limbs.^[14] Specifically, crustaceans have evolved appendages specialized for various tasks, including movement (walking/swimming), respiration and feeding, as well as threat display and for use as weapons against prey.^[14,15] Through the evolutionary process, the cuticle has been optimized, in both structure and composition, to meet the ecophysiological strains encountered by the animal.^[9,16] This natural composite displays a balance between strength and flexibility, to allow for both protection of the organism and movement.^[17]

Examples of specialization in the crustacean cuticle include the appendages of lobsters, stomatopods, and crabs. In lobster, the claws on the first pair of appendages are classified as the crusher and pincher claws owing to their functions.^[11] The claws are visibly different, with the pincher claw used to hold prey, and the crusher claw used to smash it.^[18] Similarly, the second thoracic appendage of stomatopods is highly specialized for close range combat.^[19] In some species of stomatopod, the terminal segment of this appendage (the dactyl) forms a spear-like structure, used to impale prey in an

Dr. L. K. Grunenfelder, S. Herrera,
 Prof. D. Kisailus
 Department of Chemical and Environmental Engineering
 Bourns Hall B357, Riverside, CA 92521, USA
 E-mail: david@engr.ucr.edu



DOI: 10.1002/sml.201400559

ambush style attack.^[19,20] In other species, the dactyl consists of a heavily mineralized club, which is used to smash prey (typically consisting of hard-shelled, sedentary animals such as snails) with a high energy blow.^[19,20] Another example of limb specialization is the sexually dimorphic claws of fiddler crabs. In this range of species, the male possesses a small minor claw, used for feeding, and a large major claw (4–5 times larger), used for display and combat.^[21] More general examples include adaptations for defense. Crustacean species that defend themselves by running, for example, tend to exhibit a thin and lightweight cuticle.^[9] Species that defend themselves by other means, such as rolling into a ball, have a thicker, more mineralized cuticle.^[9]

The formation of the cuticle is influenced by environmental stresses, specialized functionalities, and periodic molt events. While the general structure of the crustacean cuticle is well known, specialized elements, such as the aforementioned appendage modifications, display mechanical properties optimized to specific tasks via architecture and localized placement of organic and mineral phases.^[8,16] The hierarchical structure and mechanical properties of the crustacean cuticle have led to considerable interest from researchers in the field of biomimetics. Biomimetic processing, however, first requires an understanding of the synthesis, architecture, and chemical and mechanical properties of biological materials across all length scales. Here, we review the literature on the crustacean cuticle, presenting details of the formation and key characteristics of the cuticle, as well as the structure-function relationships observed in these biological composites. To focus the discussion, three species are examined: two decapods, the American lobster (*Homarus americanus*) and the edible crab (*Cancer pagurus*), as well as a stomatopod, the peacock mantis shrimp (*Odontodactylus scyllarus*). We conclude this review with a discussion of the development of biomimetic composites inspired by the crustacean cuticle.

2. Cuticle Structure

Before biomimetic efforts can be discussed, details of the composition and mechanical properties of the crustacean exoskeleton must be reviewed. As is common in biological composites, the crustacean cuticle displays a highly organized hierarchical structure, with features at the nanometer, micrometer and millimeter scale.^[22] This architecture allows the cuticle to respond to chemical and physical demands at various length scales.^[23,24] From a structural point of view, the cuticle can be divided into four layers. Using the commonly accepted nomenclature from Richards, these layers are, from the outermost inward: the epicuticle, exocuticle, endocuticle, and the innermost membranous layer.^[25] The outer epicuticle is the thinnest layer, consisting of proteins, lipids, and calcium salts. The main function of this waxy coating is to provide an impermeable layer to prevent water loss and provide a mechanical barrier to parasites, bacteria and fungus.^[26] The three remaining layers of the cuticle, the exocuticle, endocuticle and membranous layer, display a similar structure.^[16] The lowest degree of hierarchy in these layers, occurring at the molecular level, is an acetyl glucosamine



Lessa Kay Grunenfelder is a postdoc in the Department of Chemical and Environmental Engineering at the University of California, Riverside. Dr. Grunenfelder's background consists of a B.S. in astronautical engineering, and a masters and Ph.D. in materials science, all from the University of Southern California. During her graduate studies, Dr. Grunenfelder worked as a member of the M.C. Gill Composites Center at USC, investigating composite processing science, with an emphasis on manufacturing efficiency. Dr. Grunenfelder brings her expertise

in composites to UCR, where her research focuses on the fabrication of biomimetic composites based on structure-function relationships in biomineralized structures.



Steven Herrera graduated from the University of California, Riverside with a degree in chemical engineering in 2012, and is now a PhD student working in Bourns College of Engineering's Biomimetic and Nanostructured Materials Laboratory. As an undergraduate, he was a finalist in an international lecture competition in Hong Kong hosted by IOM3, and was actively involved in Design by Nature, an outreach program which uses university level science to encourage STEM field interest in middle school students. In his spare time he enjoys the warm southern California sun and outdoor excursions in the

majesty of nearby National Parks.



David Kisailus is the Winston Chung Associate Professor of Energy Innovation in the Department of Chemical and Environmental Engineering at University of California, Riverside. He has a B.S. in Chemical Engineering (Drexel University), a M.S. in Materials Science and Engineering (University of Florida), a Ph.D. in Materials Science and post-doctoral research in the Institute for Collaborative Biotechnologies (both at University of California, Santa Barbara). Prior to joining UCR, he was a research scientist at HRL Laboratories (Malibu, CA).

His current research encompasses crystal growth and bio-inspired materials synthesis of nanomaterials, structure-function analyses of biological materials and synthesis of biomimetic composites.

monomer, which polymerizes to form the long-chain polysaccharide α -chitin.^[8,27] At the next level are nanofibrils, formed from 18–25 crystallized chitin molecules wrapped by proteins (diameter 2–7 nm, length 300 nm).^[8,16,27] These nanofibrils aggregate to form chitin-protein nanofibers, 50–250 nm in thickness, which further organize into planar sheets.^[8,16] These sheets are then assembled in a Bouligand, or twisted plywood, structure, with each layer rotated by a fixed angle from the adjacent layer, eventually completing a rotation of 180°.^[8,27,28] These hierarchical levels are shown schematically in **Figure 3**. The organic material in the cuticle, which is in its own right a nanocomposite,^[22] is combined, in the exo- and

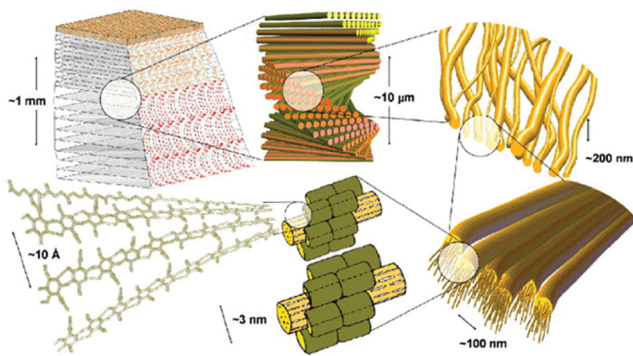


Figure 3. Hierarchical arrangement of the crustacean cuticle, from the molecular to macroscopic level. Reproduced with permission.^[30] Copyright 2007, Elsevier.

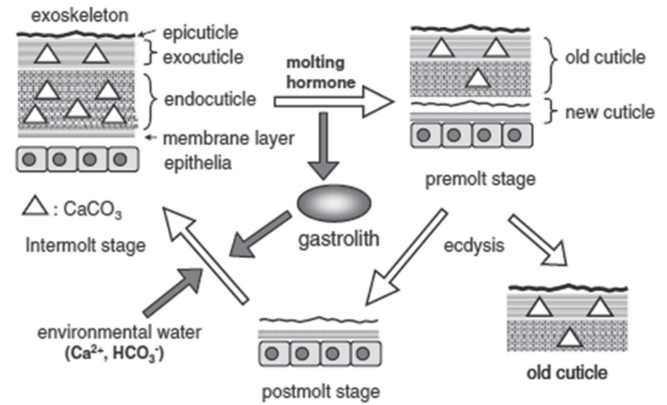


Figure 4. Schematic of the molt cycle in crustaceans. Reproduced with permission.^[34] Copyright 2007, The Company of Biologists.

endocuticle, with an inorganic matrix through a biomineralization process. The innermost membranous layer contains chitin and protein, but is not mineralized. The membranous layer is in contact with the epidermal cells during ecdysis (the period between molts).^[26,29]

The organic chitin-protein framework just described can be viewed as a scaffold, acting to template the mineral formation, controlling nucleation, growth and orientation.^[9,27,30] The mineral phase in the cuticle typically consists of amorphous and crystalline calcium carbonate and/or calcium phosphate, which fill the preformed spaces in the chitin matrix.^[8] Additional mineral phases, including crystalline magnesium calcite, are found in some species.^[9,12,31] While the organic comprises only a small percentage of the overall structure (1–5% by weight), it is a critical component, as the presence of even a small amount of organic leads to ductility and toughness of the biological composite exceeding those of the inorganic phase alone.^[1,22,32] The nanoarchitected organic and mineral phases provide both strength and ductility, leading to a damage tolerant structure. Depending on the proportions of chitin, protein and mineral in different regions of the cuticle, different properties are obtained (i.e., rigid vs. flexible, opaque vs. translucent), highlighting the versatility of the structure.^[23]

Once mineralized, the crustacean cuticle forms a rigid shell. This requires the animal to periodically molt to facilitate growth or to replace material damaged by wear or combat.^[7,29,33] The formation of the cuticle is influenced by this molt cycle. Prior to molting, a new unmineralized cuticle is secreted by the epidermal cells.^[13] The epicuticle and exocuticle are deposited before the animal molts, and the endocuticle and membranous layer are deposited afterwards.^[24,33] Following the molt, the soft cuticle is inflated with water and, over a period of days, mineralized to once again provide a hard and protective layer.^[34] A schematic of this molt cycle is presented in **Figure 4**. The hardening of the cuticle in crustaceans involves not only sclerotization (chemical cross-linking of proteins and polysaccharides), as with all arthropods, but also calcification and the addition of other inorganic minerals.^[7,9,33] Crustaceans are therefore required to regularly locate sources of calcium, which can include their surrounding environment (seawater being the primary source

for aquatic crustaceans), as well as internal calcium deposits, such as gastroliths, stored during the premolt process.^[9,33] Mineralization fundamentally consists of the precipitation of amorphous and/or crystalline calcium carbonate, or calcium phosphate, within the chitin-protein network. Crustaceans exhibit the unique ability to form, as well as resorb calcified structures,^[9] leading to a large body of research on biomineralization in crustaceans.

3. Specific Examples of Crustaceans

To emphasize general features of the crustacean cuticle, as well as highlight specialized elements, we begin this review with an overview of three commonly studied crustacean species: the American lobster, the edible crab and the peacock mantis shrimp. These organisms were chosen as a large body of literature exists on their chemical and structural organization, and they provide an overview of both common elements and specialization in the crustacean subphylum. In any discussion of the properties of the cuticle it is important to consider the biological state of the animal. This includes which stage the animal is in the molt cycle, as well as its environment and living conditions.^[11,35] Also critical to any analysis is the storage state and degree of hydration of the cuticle.^[11,35] Water content dramatically influences the mechanical properties of the crustacean cuticle. Therefore, in the studies reviewed here, samples were observed in as close to the natural state as possible. Testing procedures, however, often require an alteration of the natural conditions (specifically, hydration), which will be noted.

3.1. American Lobster

The American lobster, *Homarus americanus*, provides an ideal model system for a discussion of the key features of the crustacean cuticle. The American lobster has been studied in considerable detail, providing key insights into the development, hierarchical arrangement, and mechanical properties of the crustacean integument. An overview of the anatomy of *H. americanus* is presented in **Figure 5**. Here, we will focus on

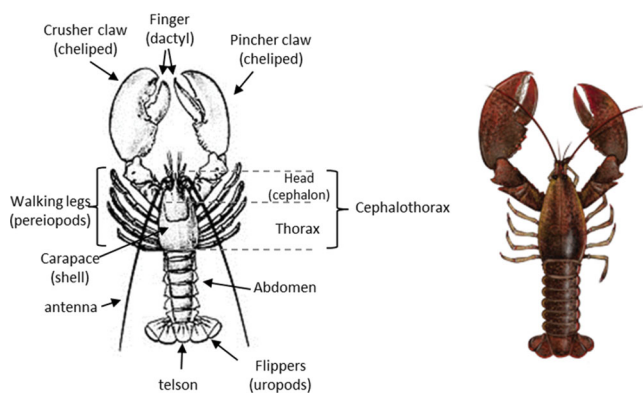


Figure 5. Details of the anatomy of the American lobster.

structure/function relationships in the lobster cuticle, drawing largely from the work of the prolific team of Raabe, Fabritius, Sachs and Al-Sawalmih.

3.1.1. Architecture

The cuticle of *H. americanus* follows the hierarchical organization detailed in Figure 3, consisting of a chitin-protein matrix, mineralized primarily by crystalline and amorphous calcium carbonate.^[11] In addition to the characteristic Bouligand structure observed in the arthropod exoskeleton, the lobster cuticle displays another important design feature common to crustaceans: a network of pore canals. These ribbon-like pores, oriented perpendicular to the cuticle surface, are elliptical in cross-section (diameter ca. 2 μm), and contain chitin fibers, which run parallel to the chitin layers that compose the rotated plywood structure.^[11,30] Pore canals make up approximately 20% of the cuticle, by volume^[36] and connect the epidermal cells to the outermost epicuticle. This indicates that the cuticle is a dynamic and living structure, capable of ion transport and self-healing.^[36] When viewed end-on, the pore canals create a honeycomb-like structure. Viewed in transverse section, they resemble twisted ribbons, as they follow the rotated plywood structure through the cuticle. The primary function of pore canals is the transport of ions to mineralize the cuticle following a molt.^[24] The well-developed pore canal system in the lobster results in a high degree of structural anisotropy.^[30]

At the nanoscale, the mineralized chitin-protein nanofibers have diameters of 50–200 nm, and are composed of nanofibrils with diameters of 2–5 nm and lengths of approximately 300 nm.^[37] Synchrotron diffraction studies have been performed to obtain information on the orientation of the crystalline α -chitin nanofibrils. Results reveal two distinct fiber textures: one parallel to the cuticle surface, forming the rotated plywood layers, and a second weaker texture perpendicular to the surface, from chitin in the walls of the pore canals.^[13,29,38] Synchrotron studies also confirm that the chitin matrix in the cuticle forms a planar honeycomb structure, with fibers connected in hexagonal arrays, rather than a linear arrangement.^[39] An out-of-plane orientation of chitin fibers is not observed in the membranous region of the cuticle, as this region does not contain pore canals^[29]

Studies of the exoskeleton of the American lobster often focus on the exocuticle and endocuticle, as these are the

regions primarily responsible for carrying mechanical loads. Of the two regions, the thin exocuticle (3–4 times thinner than the endocuticle) is more heavily mineralized, with a higher calcium content.^[18,40] The stacking height of each rotated plywood layer is smaller in the exocuticle than the endocuticle (at 10 μm per 180° rotation vs. 30 μm).^[11,18,30,41] This indicates a denser packing of layers in the hard exocuticle, and a larger difference in the rotation angle of the chitin-protein fibers. Additionally, the endocuticle has more layers per 180° rotation, resulting in a more isotropic material response.^[42] At the nanoscale, the organization and size of chitin fibers vary throughout the cuticle. Small and wide-angle X-ray scattering has revealed that overall chitin content increases from the exterior of the cuticle inward, reaching a maximum at the interface between the exo- and endocuticle.^[43] Chitin content then remains constant throughout the endocuticle, with smaller diameter chitin nanofibrils observed in this region compared to the exocuticle.^[43] The pore canal structure in the two regions also differs, with smaller pores observed in the exocuticle, further emphasizing the more dense structure of this hard outer region.^[18,40]

3.1.2. Chemistry and Phase

Energy dispersive x-ray spectroscopy studies reveal that the lobster cuticle is mineralized primarily with calcium, phosphorus and magnesium.^[30] Other elemental components of the cuticle include oxygen and carbon (oxides and organic), and trace amounts of sodium, chlorine and silicon (likely from seawater and diatoms).^[17] In the exocuticle, the mineral phase is primarily crystalline calcite, with an average crystallite size of 19 nm.^[17] This crystalline mineral is found only in the exocuticle, concentrated in a thin layer (20–50 μm) at the outermost region of the shell.^[38] The local organization and texture of calcite in the exocuticle has been investigated at the nanoscale using X-ray texture analysis and synchrotron X-ray diffraction.^[38] These studies have revealed that calcite is oriented with the crystallographic c-axis perpendicular to the cuticle surface and is associated with the out-of-plane chitin fibers in the pore canals.^[38] This preferred orientation provides stiffness, resulting in wear and impact resistance. The remainder of the structure is mineralized primarily with amorphous calcium carbonate. Similar to chitin content, the concentration of amorphous mineral is maximized at the exocuticle/endocuticle interface.^[43]

While the bulk of the lobster cuticle is mineralized with calcium carbonate, the cuticle also displays localized deposition of phosphate-based domains, mainly in the form of carbonate-apatite (an apatite in which the calcium phosphate carbonate is dominant).^[44] High resolution X-ray backscatter and electron microprobe investigations have revealed discrete regions in the cuticle which contain carbonate-apatite, previously undetected in X-ray diffraction methods because of its low quantities and discrete regional arrangement.^[12,44] In the cuticle, the presence of phosphorus is used to perform functions unattainable with calcium carbonate alone.^[44] Carbonate-apatite is found in the inner exocuticle of the lobster (**Figure 6A**).^[12,44] The exocuticle regions containing phosphorus display higher hardness and stiffness than the calcium carbonate dominated outer exocuticle.^[44] This increased

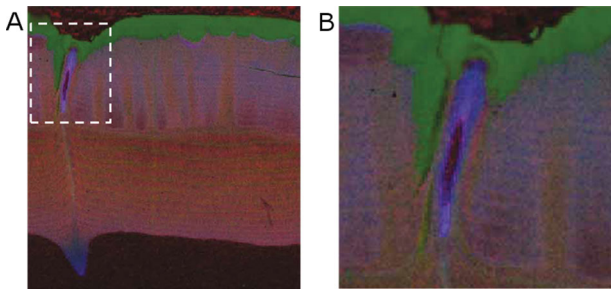


Figure 6. Energy dispersive spectroscopy false-color maps of cross sections of the lobster cuticle showing Ca (green), P (blue) and Cl (red). Reproduced with permission.^[44] Copyright 2013, Taylor & Francis.

rigidity prevents bending and cracking of the calcite layer, which would create vulnerability to microbial attack.^[44] Phosphate is also found at the boundary of the outer calcite layer and the inner region of the exocuticle, where it is thought to control the thickness of the calcite layer, hindering crystal growth to allow sufficient living space for the organism.^[44] Gland and neural canals, which are exposed to the external environment and thus susceptible to bacterial attack, are lined with apatite and carbonate apatite (Figure 6B), which provides protection from microbial action through high density and acid resistance.^[12,44] Phosphate is rare in the northern Atlantic environment (home to the American lobster),^[12] and generally, phosphorus levels in modern day seawater are less than 0.1 ppm.^[45] Crustaceans like the lobster have therefore evolved strategies to use phosphorus sparingly, to perform highly specific protective functions.^[44] This phosphate, combined with a thin external layer of calcite covered by the waxy epicuticle, provide structural support and an efficient barrier to microbial attack.^[12]

Calculations from thermogravimetric analysis (TGA), atomic absorption spectroscopy (AAS), and UV-visible spectroscopy (UV-Vis) on ball-milled cuticle samples have been utilized to determine the content of water, organic, and mineral in various regions of the integument.^[17] Mineral content and distribution varies throughout the exoskeleton increasing from the carapace (50 wt%), to the claw (60.7 wt%), and the finger (73 wt%) (refer to Figure 5).^[17] This is not surprising, given the role of each of these structures. The carapace makes up the main body of the shell, and must be flexible to allow for movement and bending of the animal. The finger is the mobile part of the cutting appendage, and is used to crush prey, requiring it to be hard.^[17] The structure and mineralization of the lobster exoskeleton, which vary throughout the structure, relate directly to mechanical performance. Fortunately, because of the large size of the lobster, and the strong interest in its mechanical performance, the properties of the cuticle have been examined from the nanoscale to the macroscale.

3.1.3. Mechanics

Fabritius et al. examined the macroscopic mechanical properties of the cuticle, carrying out tensile, compression and shear testing under both dry and hydrated conditions on test coupons from pincher and crusher claws.^[11] Under tensile

loading, hydrated samples displayed plastic deformation (0.5% yield strain and 1.8% strain at failure), while dry samples showed linear-elastic behavior and a brittle failure at a lower strain (0.7% strain at failure).^[11] Dry samples showed a higher structural stiffness (5.8–7.0 GPa) than wet samples (4.8 GPa), but a lower toughness, owing to a loss of plasticity.^[11] In a separate study, global as well as microscopic properties of the cuticle were examined using digital image correlation (DIC), a technique well suited for the analysis of heterogeneous samples.^[35] Values determined for yield strain and strain to failure in both wet and dry conditions were equivalent to those reported in reference 11. Observation of the evolution of strain during testing (via DIC) revealed step-wise crack propagation through the helicoidal architecture of the cuticle, clarifying toughening mechanisms in the hydrated cuticle that include crack deflection and crack bridging.^[35] Local strain patterns were heterogeneous in both wet and dry samples, because of material inhomogeneity such as degree of mineralization, and distribution of defects and pore channels.^[35] In both studies, the tensile behavior of pincher and crusher claws was similar.^[11,35]

Compression testing of the lobster endocuticle has revealed a highly anisotropic response in both stiffness and Poisson's ratio, owing to the honeycomb structure formed by pore canals.^[11,37] Samples tested in the normal direction displayed a large linear-elastic range, followed by the onset of plasticity.^[11,37] Samples tested in the transverse direction, however, showed a small linear-elastic region, followed by a plateau at fairly low stresses.^[11,37] Transverse samples were tested in two perpendicular directions (see **Figure 7A**). Compressive loading was shown to cause a crushing and broadening of the pore canals in one direction (direction I), and fiber bundles buckling into the pore canals in the other (direction II).^[37] Both failure modes led to large deformations.^[37] The reported Poisson's ratios in the two directions were markedly different (0.29 in direction I vs. 0.08 in direction II, in the dry cuticle).^[37] Images of compressive failure mechanisms in each direction are presented in Figure 7A.

Interesting differences were observed in fracture surfaces of compression samples tested in the normal and transverse directions. For example, samples tested in the normal direction showed cleavage in the compression plane,^[37] while those tested in the transverse direction failed at a 45 degree angle to the compressive axis (in the direction of maximum principle stress). This is similar to failure modes observed in unidirectional fiber reinforced composites^[8,37] and indicates that pore canals function not only to transport mineral, but also play a structural role in the cuticle, providing through-thickness reinforcement between laminated layers (similar to a z-pinned or a stitched composite).^[8,42] The macroscopic mechanical properties described emphasize the combined influence of a twisted plywood organization and the honeycomb structure (formed by pore canals), which results in a high in-plane stiffness and increased transverse stiffness and fracture resistance, respectively.

Variations in mechanical properties at smaller length scales have been investigated using indentation methods. Nanoindentation testing of dry samples of crusher claws have shown that modulus and hardness values vary between the

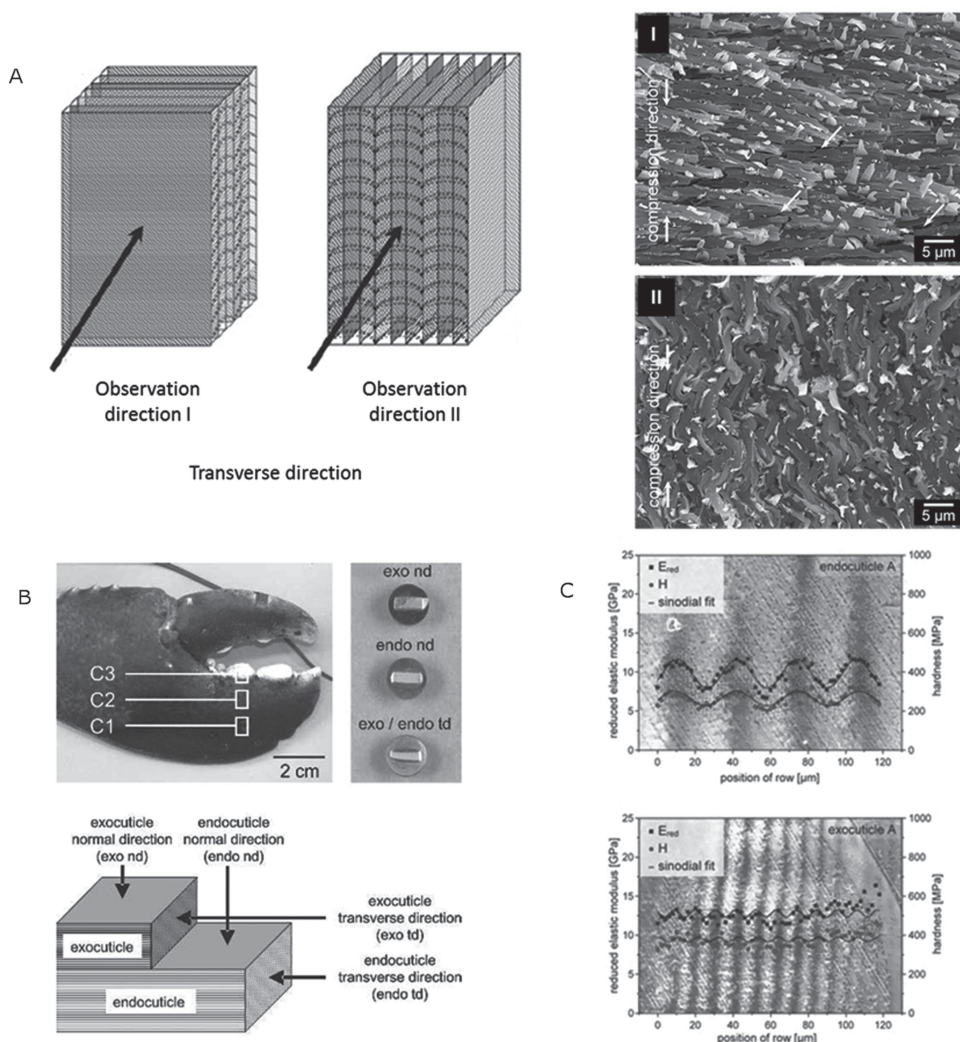


Figure 7. Mechanical properties of the lobster exoskeleton. (A) Compression testing of dry lobster cuticle samples tested in transverse directions I and II. Reproduced with permission.^[38] 2008, Wiley. (B) Locations and definition of directions of mechanical testing in the lobster claw. Reproduced with permission.^[18] 2006, Materials Research Society. (C) Nanoindentation results in the exo (top) and endocuticle (bottom), showing properties dependent on fiber direction. Reproduced with permission.^[8] Copyright 2011, Springer.

exocuticle and endocuticle, as well as in different specialized regions of the exoskeleton.^[18] For example, the exocuticle in claw locations C1 and C2 (Figure 7B), which provides structural support, has a hardness of 280–305 MPa and a modulus of 9.5–10 GPa in the normal direction.^[18] The exocuticle in location C3, however, is used for crushing prey, and is not only thicker than the exocuticle in the remainder of the shell (at 1 mm vs. 200 μm), but also exhibits twice the hardness (545 MPa) and stiffness (24 GPa).^[18] The exocuticle, as expected, shows higher hardness and modulus than the endocuticle (by approximately 15% and 20% in the normal direction).^[18] Nanoindentation across periods in the exocuticle and endocuticle has revealed an oscillation in hardness and modulus, which line up with the periodicity of the Bouligand structure and stem from the rotated fiber directions in the cuticle (Figure 7C).^[8] Microindentation studies have also proven the existence of a mesoscopic structural gradient through the thickness of the cuticle, with mechanical properties dictated by changes in stacking height and degree

of mineralization.^[41] A hardness gradient exists within the densely rotated exocuticle itself (130 MPa at the surface to 270 MPa near the endocuticle), followed by an abrupt transition that occurs between the exocuticle and endocuticle, with the latter displaying reduced hardness (30–55 MPa).^[41]

The influence of nanoscale morphologies on mechanical performance is difficult to examine using experimental approaches, as it is challenging to obtain mechanical and structural data at the nanometer scale.^[46] For this reason, simulation-based approaches using multiscale modeling have been applied to investigate properties from the atomistic to macroscopic scale.^[40,46] The mechanical properties, microstructure, and crystallographic orientation of the lobster cuticle have been extensively examined, allowing analytical models to be developed and validated.^[46] Using *ab initio* calculations at the nanometer scale (where experimental results are lacking), Nikolav et al. have utilized bottom up approaches with micromechanical models and homogenization methods to examine hydrated lobster cuticle in a range

of length scales (from 10^{-9} to 10^{-3} m).^[46] This approach has been employed to ascertain previously unknown details of the cuticle. One such discovery relates to the microstructure of the mineral-protein matrix, which is reported to be a symmetric cell material of spherical calcium carbonate particles in a protein matrix.^[46] Symmetric cell materials are a highly optimized structure for maximizing stiffness, and are as of yet not attainable using synthetic processes.^[46] Multiscale models have shown reasonable agreement with global properties observed in experimental work, and have validated toughening mechanisms of the cuticle, including the crack resistance and energy dissipation of the Bouligand structure as well as the influence of degree of mineralization on mechanical performance.^[46] Predictions of the change in mechanical properties of the cuticle as a function of material and design parameters (specifically properties and volume fractions of chitin, mineral, and protein) have further revealed that the natural composite is highly optimized across all length scales, exploiting the full potential of each constituent component.^[40]

The lobster cuticle is a complex hierarchical biological composite, with a heterogeneous structure and properties defined not only by the properties of the constituent materials (chitin fibrils, biominerals), but also heavily influenced by architecture. The cuticle, which shows anisotropic response at all length scales, is optimized to relevant loading scenarios through changes in the spatial orientation of chitin fibers, as well as the degree of mineralization in different regions.^[11] The structure displays a multi-layer design, with a hard outer layer adapted to resist compressive loads.^[46] The underlying amorphous phase is more elastic and acts to dissipate impact energy.^[38] Bulk compression testing reveals the resistance to deformation of the structure when loaded in the normal direction, a situation which would occur during attack by a predator.^[37] Results of indentation testing emphasize the high degree of anisotropy present in the lobster cuticle, as well as the influence of mineralization on mechanical properties, and the specialization of different regions for specific functions. From a mechanical point of view, the twisted plywood arrangement of the cuticle, and the honeycomb structure created by reinforced pore canals, represents a porous yet stiff natural material, optimized to resist external loads and protect the animal within.

3.2. Edible Crab

The edible crab, *Cancer pagurus*, was first described by Carl Linnaeus in 1758, and classified with all other arthropods as belonging to his class of “Insecta” (the full name of the species is often listed as *Cancer pagurus Linnaeus*).^[47] Since that time, other researchers have observed the species in detail, beginning with pioneering work by Drach in 1939.^[48] In the 1970s, Hegdahl et al. added detailed studies on the endocuticle,^[49] exocuticle,^[50] and epicuticle^[51] regions of the integument. An additional series of publications by Welinder during the same decade provided detailed information on the specific components of the cuticle, including analysis of amino acid and protein compositions.^[52–54] More recent works by

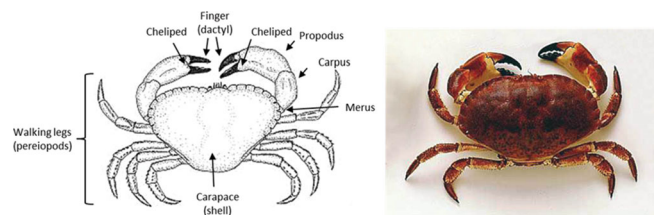


Figure 8. Details of the anatomy of the edible crab.

Fabritious and his team included mechanical property analysis of the exoskeleton of *Cancer pagurus*.^[16,17]

3.2.1. Architecture

An overview of the edible crab is presented in **Figure 8**. Detailed studies of the dorsal carapace of the organism have revealed regional differences in the structural organization and mineralization, resulting in variable mechanical properties. The epicuticle of *C. Pagurus* is approximately $5\ \mu\text{m}$ in thickness, consisting of a $1\ \mu\text{m}$ hard outer layer, with a $3\text{--}4\ \mu\text{m}$ thick underlying layer containing pore canals oriented perpendicular to the cuticle surface.^[16,51] These pore canals, likely continuous throughout the cuticle, end at the exterior of the epicuticle in mineralized spines, measuring approximately $18\ \mu\text{m}$ in length.^[51] Underneath the epicuticle is the exocuticle, which displays the characteristic Bouligand structure found in other arthropods, and has a stacking height of approximately $1.3\ \mu\text{m}$ ^[16] that increases in the proximal exocuticle. Pore canals with a diameter of approximately $300\ \text{nm}$ are observed, which do not contain organic fibers or mineral particles.^[16] The organic fibers in the exocuticle are in all cases associated with mineral, and do not display a clearly defined fiber structure.^[16]

Near the interface of the exocuticle and endocuticle, large and randomly oriented channels are observed running perpendicular to the pore canals.^[16] A sharp transition occurs between the exocuticle and endocuticle, observed in optical microscopy as a thin dark line, though the pore canals are continuous across the interface.^[16] This transition is organic-rich,^[16] and may prevent the propagation of cracks across the interface. The endocuticle displays a pitch-graded structure, with the stacking height of rotated plywood layers decreasing from the exterior inward. The organic chitin-protein matrix in the endocuticle is formed by fibers $70\ \text{nm}$ in diameter, composed of fibrils with a diameter of $7\ \text{nm}$.^[16] The mineral phase forms a solid tube, surrounding individual chitin protein fibers, with neighboring tubes fused together.^[8] These mineral tubes are composed of individual mineral granules measuring 20 to $50\ \text{nm}$.^[16] The structure is penetrated regularly by a twisted ribbon arrangement of pore canals with an elliptical cross section, measuring approximately $1\text{--}2\ \mu\text{m}$ \times $0.5\ \mu\text{m}$, with the major axis of the ellipse parallel to the Bouligand layers.^[16,49] Here, organic tubes are observed running within the pore canals, as are mineralized fibers, which are located on opposite ends of the long axis of the elliptical pores.^[16,49] These fibers provide structural reinforcement along the length of the canals. Details of the crab ultrastructure, revealed through SEM analysis of fractured samples, are presented in **Figure 9A**.

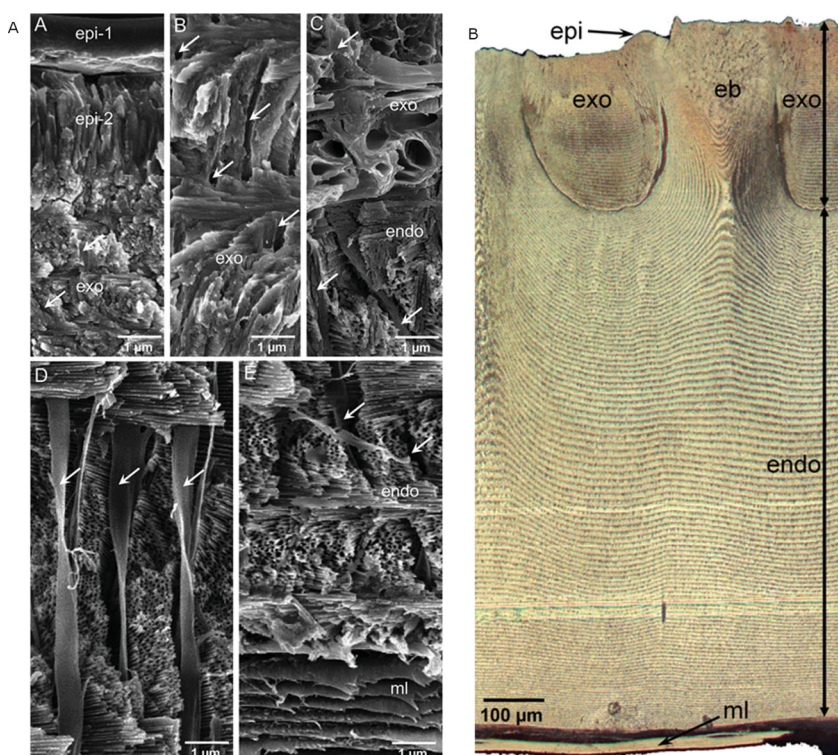


Figure 9. (A) Optical micrograph of the crab cuticle showing the epicuticle (epi), exocuticle (exo), endocuticle (endo), endocuticular bulges (eb) and the inner membranous later (ml); (B) SEM images of fractured sections revealing the ultrastructural detail in each region of the cuticle. Reproduced with permission.^[16] Copyright 2012, Birgit Zoglmeier.

A unique set of features observed within the edible crab exoskeleton are regions of the endocuticle, which extend into the exocuticle, forming irregularly spaced endocuticular bulges, shown in Figure 9B.^[16,48,49] These bulges result in visible swellings on the exterior of the shell.^[51] Structurally, the exocuticle composes roughly 20–25% of the total thickness of the shell (in the regions not interrupted by endocuticular bulges),^[16,50] while the endocuticle makes up the remaining 75% of the structure.^[49] Near endocuticular bulges, adjacent rotated plywood layers bend toward the cuticle surface.^[49] The Bouligand structure within the bulge regions is altered, rotating around a horizontal, rather than vertical axis.^[16] Pore canals in these regions, therefore, run parallel to the twisted plywood layers, and thus propagate in a straight line, with no observed rotation.^[16] The rotated plywood structure in the exocuticle is not interrupted by the bulges, but is rather continuous, simply fluctuating in stacking height and rotation.^[16] The centers of the endocuticular bulges have a V shape (see Figure 9B) and appear heavily mineralized in fractured samples.^[16] Pore canals in this region are small and commonly filled with mineral.^[16]

3.2.2. Chemistry and Phase

Regional analysis has revealed a range of mineral phases in the crab exoskeleton. The epicuticle, as in most crustaceans, is a waxy layer, and is devoid of chitin fibers, though amorphous calcium carbonate mineral particles are present within the vertical pore canals.^[16,48,51] The exocuticle is divided, from a mineralization standpoint, into three

distinct regions. X-ray powder diffraction (XRD) reveals that the outermost region of the exocuticle is mineralized with 25 nm crystallites of calcite,^[17] though the presence of magnesium in the EDS signal in this region indicates that the mineral phase may be magnesium calcite.^[16,17] In the central region of the exocuticle, phosphorus signals are detected by EDS, with Raman spectroscopy confirming the presence of phosphate.^[16] Amorphous calcium carbonate and magnesium are also observed in the central region, which may suggest the presence of a $\text{Mg-PO}_4\text{-CO}_3$ phase.^[16] In the final region of the exocuticle, closest to the endocuticle interface, calcium dominates the EDS spectra, with only low quantities of magnesium and phosphorus detected.^[16] Raman and XRD reveal the mineral phases present to be amorphous calcium carbonate along with hydroxyapatite.^[16,17]

Despite a uniform appearance in optical micrographs, Raman data (Figure 10) shows that the endocuticle differs in chemical composition in the regions located directly below the exocuticle.^[16] Magnesium calcite is observed in the bulk of the endocuticle, though no calcite signal is present in the regions below the exocuticle, which are likely composed of amorphous calcium carbonate (Figure 10B).^[16] The central, V shaped regions of the endocuticular bulges are heavily mineralized with magnesium calcite, displaying a low organic signal.^[16] Carotene is also detected throughout the cuticle (Figure 10E), potentially serving as a pigment.^[16]

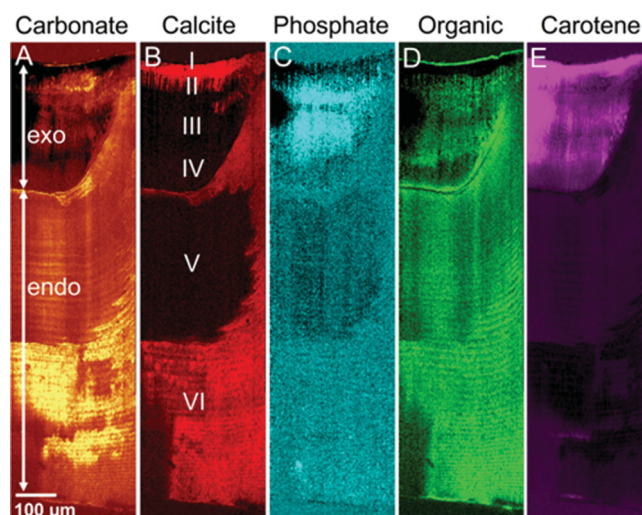


Figure 10. Raman spectral maps of the crab cuticle showing the distribution of (A) carbonate, (B) calcite, (C) phosphate, (D) organic, and (E) carotene. Reproduced with permission.^[16] Copyright 2012, Birgit Zoglmeier.

3.2.3. Mechanics

Nanoindentation maps have been performed, providing information on the local mechanical properties in different regions of the cuticle. The lowest hardness and stiffness values in the crab exoskeleton (5 GPa and 100 MPa) are observed in the phosphorus-rich central region of the exocuticle, with the outermost calcitic region showing the highest values for the exocuticle.^[16] The endocuticle has an average stiffness of 10 GPa and hardness of 200 MPa, while the heavily mineralized V-shaped regions of the endocuticular bulges display a four-fold increase in stiffness and hardness, at 40 GPa and 1200 MPa, respectively.^[16] In some areas of the cuticle, the hardness and modulus data clearly reflect the rotated plywood patterns, indicating a correlation between mechanical properties and the orientation of chitin fiber layers.^[16]

While much of the research effort on *Cancer pagurus* has focused on the carapace, other regions of the shell have also been examined. As with the lobster cuticle, thermogravimetric analysis was performed on ball milled samples of various regions of the cuticle of *Cancer pagurus*.^[17] Mineral content was reported to be highest in the finger (88.6 wt%), followed by the claw (76.7 wt%), with the lowest mineral content in the carapace (71.6 wt%).^[17] These values are consistent with the trend reported by Welinder, who showed an approximate 10% increase in calcium salt content in the claw vs. the carapace.^[52] These results indicate optimization of the claw region of the cuticle to provide the mechanical strength necessary for the animal to break apart the shells of its prey.^[52]

Overall, the structure of the crab exocuticle is optimized to withstand significant mechanical loads, particularly compressive forces applied perpendicular to the shell surface from predators. In addition to the rotated plywood structure and mineral reinforced perpendicular pore canals also described in the lobster cuticle, alternating regions of hard endocuticular bulges and softer regions of the distal exocuticle are thought to provide protection against predators with sharp appendages, such as the beaks of cephalopods.^[16] The endocuticular bulges also act as strengthening pillars in the structure, transferring compressive loads to more proximal regions of the endocuticle. The abrupt transition from the exocuticle to the endocuticle results in crack deflection.^[16] This transition, along with the rotated plywood organization of the endocuticle, prevents damage propagation through the structure.

3.3. Peacock Mantis Shrimp

While this review, thus far, has focused on decapod crustaceans, the final species we will discuss is a more aggressive predator, the stomatopod *Odontodactylus scyllarus* (**Figure 11**). While lobsters and crabs crush shells with cyclic loads of low peak force over long time periods (using a crushing mechanism), smashing stomatopods, such as *Odontodactylus scyllarus*, break shells with a high peak force, delivered over a short time (using a hammer mechanism).^[55] The biological hammer employed by the stomatopod is a heavily mineralized dactyl club which makes up the terminal segment of the second thoracic appendage (raptorial appendage).^[19]

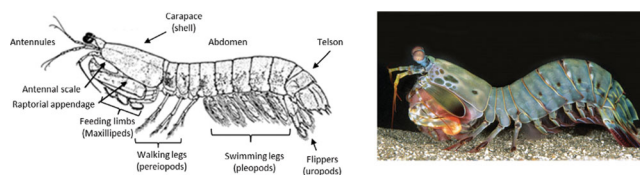


Figure 11. Details of the anatomy of the peacock mantis shrimp. Images reproduced with permission from Roy Caldwell.

The peacock mantis shrimp can deliver a strike lasting only a few milliseconds, with the speed of the strike resulting in cavitation between the club and the shell surface.^[55] The collapse of cavitation bubbles results in a second impact to the prey. Using force transducers, high-speed video, and acoustic analysis, Patek et al. measured the impact and cavitation forces produced by the strike of the stomatopod dactyl club. On a flat steel impact surface,^[55] using a 3-axis force sensor, limb impact forces with an average of 693 ± 174 N were recorded, followed closely (0.5 ms) by cavitation forces of 348 ± 116 N. Individual striking events with impact forces exceeding 1000 N were recorded.^[55] By utilizing a hammer mechanism, the stomatopod is able to generate forces thousands of times its own body weight, a feat not attainable by an animal of similar size through a crushing mechanism. Advanced imaging techniques have shown that the strike of *Odontodactylus scyllarus* reaches speeds of 14–23 m/s, angular speeds of 670–990 rad/s, and accelerations of 65–104 km/s²,^[56] making the stomatopod strike one of the fastest known animal movements.^[57]

To withstand the strike force exerted by the stomatopod, the dactyl club itself must be strong and tough. While the dactyl club gradually displays pitting from cavitation bubbles and microcracking from impact, the structure can withstand thousands of repeated impact events without catastrophic failure, and maintain structural integrity until it is replaced in periodic molting events.^[19,58] Examination of the dactyl of the smashing stomatopod *Gonodactylus* by Currey in the early 1980s,^[58] and recent work on *Odontodactylus scyllarus* by the Kisailus group,^[19] have shed light on how the cuticle in the club is optimized to withstand impact damage.

3.3.1. Architecture

The raptorial appendage of the stomatopod (**Figure 12A**) consists of multiple parts. The largest segment is referred to

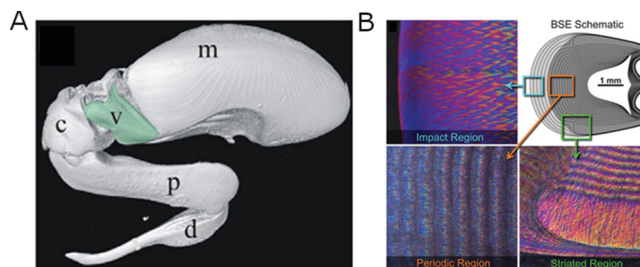


Figure 12. (A) The stomatopod raptorial appendage, showing the location of the merus (m), meral-V (v), carpus (c), propodus (p) and dactyl (d). Reproduced with permission.^[59] 2009, The Company of Biologists. (B) A schematic of a transverse cross-section of the dactyl, highlighting the three distinct regions with optical micrographs. Reproduced with permission.^[19] Copyright 2012, AAAS.

as the merus. The next, slightly smaller segment is the carpus, which is followed by the elongated propodus. The final segment, the dactyl, is also elongated and folds into a groove under the propodus.^[59] During a strike, the dactyl remains folded into the propodus and the prey is struck by the blunt dactyl heel.^[59] It is the specialized structure of the merus that provides the exoskeletal power amplification required to generate the devastating strike of the stomatopod. This amplification facilitates the rapid acceleration of the club, which would not be attainable through muscle contraction alone.^[57,60,61] An analog to this amplification process was presented by Patek, who correlated the system to a crossbow. With the crossbow, the human arm muscle works to gradually load and store energy in the bow, after which the trip of a latch results in the rapid release of the stored energy, and propulsion of the arrow.^[61]

Microcomputed tomographic analysis of the entire body of *Odontodactylus scyllarus* has revealed that the dactyl club is the most electron-dense region of the entire stomatopod exoskeleton, and thus the most heavily mineralized.^[19] When viewed in transverse cross section, the club can be divided into three distinct regions, termed impact, striated, and periodic (Figure 12B).^[19] BSE micrographs reveal that the outer impact region, which is the exocuticle of the stomatopod club, is the most heavily mineralized region of the club.

The endocuticle of the stomatopod club is composed of the periodic and striated regions. The periodic region is so named as it displays the characteristic Bouligand structure common to the arthropod exoskeleton. The pitch of the rotated plywood layers in the periodic region decreases from the exterior inward, and is greatly expanded compared to other species, with a pitch length of as much as 100 μm near the impact region.^[19] The Bouligand structure of the periodic region follows the contours of the club.^[19]

A unique feature of the stomatopod club is the striated region, which shows a much different organization of chitin-protein sheets. In this region, aligned fiber bundles are observed, oriented perpendicular to the transverse cross section.^[19] Here, the chitin-protein sheets described in Figure 3 are stacked with a single fiber orientation, rather than a helicoidal architecture. These aligned fiber sheets form a circumferential band around the club, preventing lateral deformation, and reducing the maximum principle strain within the bulk of the club during a strike.^[19] This striated region of aligned fiber bundles is an evolutionary adaptation specific to the dactyl club, providing resistance to catastrophic damage from high velocity impact events. Though not reported in the literature, investigations by the authors have confirmed the existence of a pore canal network in the stomatopod club, which rotates with the helicoidal layers in the periodic region, and runs straight in the aligned striated region.

3.3.2. Chemistry and Phase

The exocuticle of the stomatopod dactyl club, which forms the outermost impact region, is heavily mineralized. Past investigations of a smashing stomatopod club by Currey have shown that this region is mineralized primarily by calcium phosphate.^[58] Later synchrotron microdiffraction data presented by Weaver et al. reveal that this phosphorus rich phase is crystalline hydroxyapatite, with the (002) lattice planes oriented parallel to the impact surface.^[19] Similar to observations in the edible crab, there is a sharp transition between the impact region (exocuticle) and the periodic region, which makes up the bulk of the endocuticle. This transition is marked by a step-like decrease in calcium content.^[19] The phosphorus content, on the other hand, decreases in a gradient-like fashion, accompanied by an increase in magnesium and carbon.^[19] The endocuticle of the club is mineralized with a mixture of amorphous calcium phosphate and amorphous calcium carbonate, with magnesium present and assumed to help stabilize the amorphous phase (Figure 13A).^[19]

3.3.3. Mechanics

Nanoindentation scans have been performed to probe the micromechanics of the dactyl club. In general, the extent of mineralization in each region of the club is directly related to mechanical performance, with the phosphorus-rich regions of the structure displaying the highest hardness and modulus values, and hydration level influencing properties more strongly in less mineralized regions.^[19,58] Indentation maps (Figure 13B) show that the outer impact region is the stiffest and hardest region of the club (modulus of 65–70 GPa, hardness of 3–4 GPa).^[19] There is a decrease in mechanical properties observed from the exocuticle inwards to the periodic

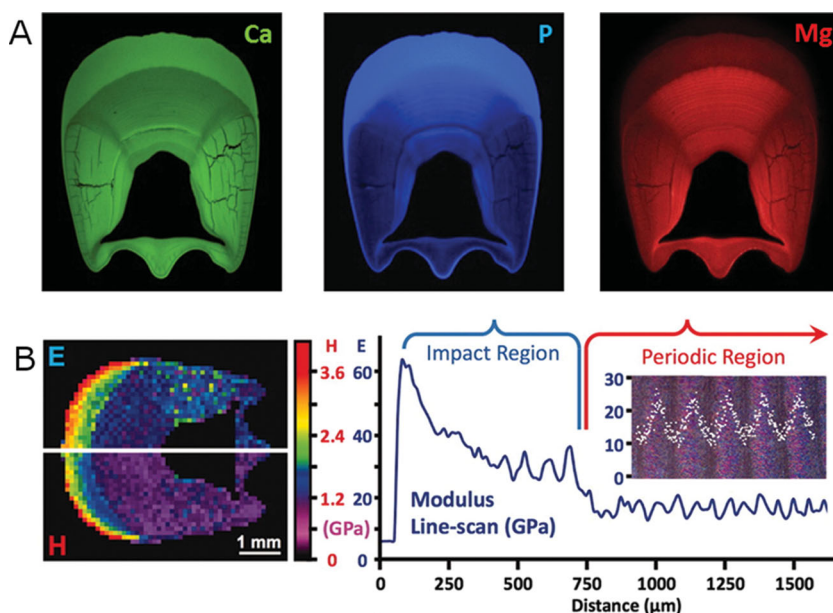


Figure 13. (A) Elemental analysis of the stomatopod dactyl club, showing the distribution of Ca, P and Mg; (B) Nanoindentation results revealing the hardness and modulus in the club, accompanied by a line scan showing an initial decrease in modulus moving into the periodic region, followed by a modulus oscillation. Reproduced with permission.^[19] Copyright 2012, AAAS.

region, along with a cyclic modulus that aligns with the rotated plywood layers, with maximum and minimum values of 10 and 25 GPa.^[19]

The damage resistant characteristics of the stomatopod dactyl club are a result of a combination of structural features and localized mineralization.^[19] As a first line of defense, the club has an outer impact region, characterized by increased hardness through a higher degree of crystallinity, as well as a specific orientation of hydroxyapatite crystallites. Moving toward the interior of the club, additional toughening features are observed. The helicoidal structure of the chitin matrix in the periodic region results in a rotating crack front, leading to a greater dissipation of energy during impact and crack propagation. The sharp transition reported between the impact surface and the bulk of the impact region results in a modulus mismatch. An internal crack propagating to the impact surface will encounter this mismatch, and likely be deflected at the interface, preventing catastrophic failure. Lastly, the aligned fibers of the striated region, which wrap the circumference of the club, prevent lateral deformations and provide compressional and torsional stiffness to the club during impact.

3.4. Unifying Features and Specialization

The cuticles of the three species discussed reveal universal themes common across the crustacean subphylum, as well as highlight features evolved for specific functions. As a general description, the crustacean cuticle consists of a rotated plywood structure, formed from a chitin-protein organic template, mineralized by calcium carbonate and calcium phosphate. The cuticle contains a network of pore canals, which create a honeycomb structure. Common features observed are a hardened (more mineralized) outer region for impact and abrasion resistance, accompanied by a sharp transition between the exo- and endocuticle to prevent crack propagation. As highlighted in the previous discussion, however, the cuticle is a complex system, evolved in each species based on differences in habitat as well as defense and attack strategies. Key examples of this specialization include the endocuticular bulges observed in *Cancer pagurus*, which optimize the shell to withstand perpendicular compressive loads, and the striated region of aligned chitin fibers in *Odonotodactylus scyllarus*, which allow the dactyl club to withstand high energy impact events. More subtle variations are also observed. Lobsters, for example, are mobile animals who swim away from predators, resulting in a lighter and less mineralized cuticle.^[17] Crabs, on the other hand, tend to burrow in the sand or cling to the ground upon attack, and have thus evolved a thicker and more heavily mineralized shell.^[17] Both lobsters and crabs utilize a crushing mechanism, with mineralized claws optimized for crushing prey. Stomatopods, in contrast, are a smaller animal, and utilize an aggressive hammer mechanism to attack prey.^[55] While the dominant mineral component in crustacea is calcium carbonate, most commonly found as ACC or calcite, the three species examined reveal an optimized incorporation of phosphorus. Lastly, crustaceans showcase the ability to precisely control

the phase and location of mineral in the cuticle to optimize mechanical properties, a fact that has driven a considerable amount of research in the field of biomimetics.

4. Biomimetic Composites Inspired by the Crustacean Cuticle

The properties observed in the exoskeleton of crustaceans have been the inspiration for biomimetic efforts. The term “biomimetic” can refer to processing routes and/or design strategies, both of which we will discuss here. Biomimetic processing routes have been explored for the self-assembly of organic scaffolds, as well as the mineralization process. Biomimetic design strategies have been implemented in both mineral and organic systems as well as high performance composite materials.

The controlled mineralization observed in the crustacean cuticle, in particular the stabilization of the amorphous phase, has resulted in biomimetic mineralization efforts. In the field of biomineralization, the processing and design strategies employed in nature are applied to the fabrication of materials with desirable properties. During this processes, information is gleaned regarding biological phenomena. We will first discuss biomineralization in crustaceans, followed by achievements in biomimetics, from assembly of organic scaffolds, to controlled mineralization of calcium carbonate. Beyond this, the development of ceramic and fiber-reinforced composites inspired by the crustacean cuticle will be discussed.

4.1. Biomineralization

The biomineralization process is one of the most remarkable features of biological composites. Through biomineralization, organisms control the specific locations of mineral nucleation and growth, the phase of the mineral, and the size, shape and orientation of the crystal.^[62–64] This control of mineral in the crustacean cuticle, as with other biological systems, is afforded by the use of organic templates.^[62] In crustaceans, the template consists of an insoluble framework macromolecules of α -chitin, which combine with soluble macromolecules to form a chitin-protein complex.^[65] The soluble macromolecules are largely acidic and negatively charged (anionic).^[45,66,67] They include proteins and glycoproteins rich in aspartic acid, glutamic acid and serine, as well as polysaccharides that are often sulfated or phosphorylated.^[65,68] Often, magnesium and phosphate ions are also present as additives, working together with the proteinaceous macromolecules and low-molecular weight components of the organic matrix to template and control mineral nucleation and growth.^[66] The organic scaffold and inorganic material form complex nanoscale composite structures.^[45]

The periodic molt cycle is an integral part of growth for a crustacean, during which the biomineralization process is critical. This molt cycle necessitates the resorption of mineral, as well as the incorporation of pore canals in the cuticle to allow for the transport of ions to rapidly deposit mineral in the new exoskeleton. A cellular hypodermis, underlying the

cuticle structure, is responsible for the synthesis of the new exoskeleton.^[9] Prior to the molt, the hypodermis partially resorbs organic and inorganic materials from the existing cuticle.^[69] The epicuticle and exocuticle are formed prior to the molt, but despite containing calcium and carbonate ions, do not harden until after the organism molts and swells with water.^[69] This control over mineralization is a result of changes in the protein composition of the cuticle following ecdysis (molt).^[69] After a molt, the new cuticle is mineralized, with nucleation and growth beginning in the most external region of the exocuticle.^[24]

The molt cycle highlights the importance of amorphous mineral phases in Crustacea. Crustaceans must locate sources of calcium to mineralize the new cuticle after ecdysis. While the primary source for marine species is seawater, calcium storage mechanisms are also common.^[9,45] The American lobster, for example, develops gastroliths for temporary calcium storage.^[7] Gastroliths form in the stomach of the animal, during the premolt period.^[70] Gastroliths are composed primarily of amorphous calcium carbonate, along with a small content of proteins and polysaccharides (chitin), which likely help to stabilize the amorphous phase. These structures continue to enlarge, triggered by a molting hormone, until the molt occurs. After the molt, they are digested to provide calcium carbonate to harden the new exoskeleton.^[70] For the edible crab, calcium storage, typically in the form of calcium phosphate, occurs in the hepatopancreas digestive gland, which may also play a role in detoxification.^[9] Calcium storage involves an amorphous phase, as it is more soluble than its crystalline counterpart, allowing the mineral to be partially dissolved during the molt cycle and readily available for reuse.^[65,71–73] This amorphous material is found both as a transient phase, crystallizing after deposition, and as a stable phase in the mineralized exoskeleton.^[72,74–77]

4.2. Biomimetic Scaffolds: Liquid Crystalline Assembly of Chitin

The overarching design motif in the arthropod phylum is the rotated plywood, or Bouligand structure. The helicoidal architecture and optical properties in the rotated plywood regions of the crustacean cuticle are reminiscent of chiral nematic liquid crystals, indicating the possibility of a transient liquid crystalline phase during cuticle formation.^[28] In a chiral nematic, or cholesteric liquid crystal, a handed twisting occurs, with a finite angle of rotation between adjacent molecules. Using this observation as inspiration, efforts have been undertaken to recreate biological architectures and natural self-assembly in the laboratory, through *in vitro* ordering of highly anisotropic rods (length \gg diameter) of various polysaccharides and proteins.^[78] Most relevant to a discussion of the crustacean cuticle, are such efforts involving α -chitin. A key discovery enabling this field of research was the observation by Marchessault et al., who found that acid-hydrolyzed chitin will spontaneously disperse into rod shaped particles.^[79] As described by Onsager, these long filaments, when suspended in solution, are likely to form an anisotropic assembly at high concentrations.^[80]

Using purified chitin from crab and shrimp, Marchessault and colleagues have prepared colloidal suspensions of chitin under acid hydrolysis.^[81–84] At a critical concentration, these solutions yield a two phase system, consisting of an isotropic phase, along with an ordered nematic phase. The material maintains order when slowly dried to a solid film, and has been imaged using TEM, revealing the characteristic nested arc pattern observed in the crustacean exoskeleton (Figure 14A, B).^[83]

Detailed investigations have been carried out to examine the influence of ionic concentration, pH, and chitin content on the formation of a chiral phase. Measurements of zeta potential have been performed, showing that chitin crystallites are positively charged.^[81] The self-assembly and stability of colloidal suspensions is attributed to stabilizing positive charges on the crystallites, which arise from protonation of amino groups, leading to electrostatic repulsion.^[83] The influence of a change in the surface charge of the chitin on the formation of the chiral phase has been examined.^[82] In one study, the charge was altered from positive to negative through N-sulfonation of the surface amino groups.^[82] The extent of N-sulfonation and the pH of the suspension were shown to influence the colloidal behavior of chitin crystallites.

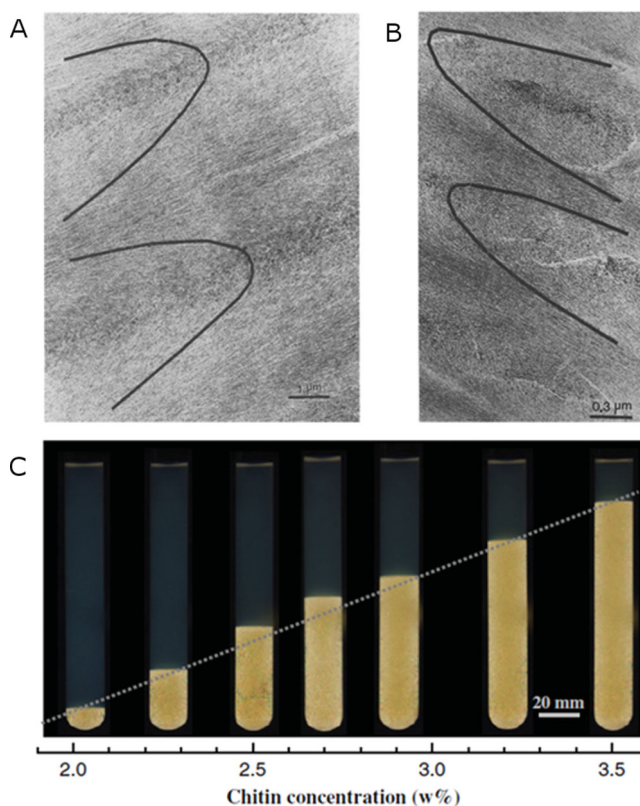


Figure 14. (A) TEM of ultra-thin sections of (A) a film formed from slow evaporation of a chiral nematic mesophase of chitin crystallites, and (B) shrimp shell, showing the nested arc pattern characteristic of a cross-section of helicoidally arranged fibers. Reproduced with permission.^[83] 1993, Elsevier. (C) Polarized light images of suspensions with increasing chitin concentration, showing the isotropic phase (top, dark) and nematic phase (bottom, bright). Reproduced with permission.^[78] Copyright 2006, IOPscience.

When a critical surface charge density ($\approx 0.10 \text{ e/nm}^2$, where e is elementary charge) and a critical ratio of N-sulfonated amino groups to amino groups ($S/N > 3$) was obtained, chiral nematic phases were formed.^[82] In a separate study, surface charge density was controlled through NaOH deacetylation.^[84] This work revealed that the boundary concentration for phase separation increases with increasing surface charge, a relation opposite to that predicted theoretically. This arises as a result of the contribution of the chitin crystallites themselves to the ionic strength of the solution.^[84] The rheological properties of suspensions have also been probed,^[85] and it has been demonstrated that chiral phases cannot form when viscosity is too high, which can occur after extended alkali treatment.^[84]

Additional experiments, performed by Belamie et al., have shown an increase in the proportion of the chiral phase as a function of chitin concentration (Figure 14C).^[78] However, at concentrations exceeding 13 wt% chitin, no chiral nematic ordering was observed.^[79] In another experiment, chiral suspensions were prepared from purified chitin fibers extracted from crab shells, with an average length of $260 \pm 80 \text{ nm}$ and diameter of $23 \pm 3 \text{ nm}$.^[86] The influence of pH and ionic concentration on phase separation were investigated through varying HCl concentrations and the addition of NaCl. This work revealed that a biphasic system will form only under specific HCl and chitin concentrations, and that ionic strength has a strong influence on phase separation.^[86] As the NaCl concentration is increased, the electrical double layer is compressed, and particles can be packed more closely, leading to an increase in the critical concentration for phase separation.^[81] In the coexistence domain, when both the isotropic and chiral phases are present, increasing the chitin concentration was shown to yield a reduced pitch length (pitch varied from $27.5 \pm 3.5 \mu\text{m}$ to $140 \pm 17 \mu\text{m}$ depending on concentration) and a linear increase in the concentration of the nematic phase.^[86] These studies suggest that tailored phases can be produced by controlling solution concentration, ionic strength, and pH value, which is a known strength of biological systems.

Similar experiments have been performed on chiral nematic ordering of other polysaccharides, notably cellulose. These studies, many of which were reviewed by Gray,^[87] have shed additional light on the conditions influencing pitch and twist sense in chiral phases. For example, the direction of the chiral nematic axis was shown to be controllable by the application of a strong magnetic field.^[88] Cholesteric liquid crystalline structures have also been spontaneously formed under acidic conditions, with high concentrations (80 mg/ml) of the protein collagen, which is found in vertebrate tissue and compound bone. These structures maintained their shape to neutral pH in a gel state when neutralized under ammonia vapor.^[89] Investigations of chiral nematic ordering of polysaccharides provide the tools needed to produce ordered materials with structural control on multiple length scales, which maintain their shape upon dehydration. These biomimetic materials, with the potential for controlled pitch, have application possibilities of their own, but can also be associated with a mineral phase for further functionality.

4.3. Biomimetic Mineralization of CaCO_3 for Nanoscale Organic-Inorganic Composites

Biomimetic mineralization, using an organic phase to template mineral growth, is a rich field of study, and the interested reader will find a range of publications on the topic.^[45,63,90–93] The goal of biomimetic mineralization is to achieve nanometer scale organic-inorganic composites with controlled properties using environmentally benign synthesis pathways. As it is most relevant to the crustacean cuticle, we will primarily limit this section to a review of biomimetic mineralization of calcium carbonate. As has been pointed out by Gower, it may seem strange to focus research efforts on the mineralization of CaCO_3 , as the material itself has few commercial applications.^[76] This simple model system, however, provides insight into the biomineralization process, and creates a knowledge base that can translate to the synthesis of other materials at atmospheric temperature and pressure.^[76] Our discussion will address multiple routes toward biomimetic mineralization of calcium carbonate: from chitin-based scaffolds to synthetic polymer templates. We will also highlight the importance of additives (both biological and synthetic) in controlling mineralization, as well as biomimetic efforts to stabilize an amorphous mineral phase. Additional topics addressed in this section are chitin-based composites for biomedical applications and biomimetic tanning of organic material.

4.3.1. Chitin and Chitosan Scaffolds

Critical aspects of the toughness and strength observed in biological materials stem from nanoscale interactions among mineral and organic (specifically chitin and protein) components.^[94] Chitin has a low solubility, making it difficult to work with. For this reason, biomimetic composites are often fabricated using chitosan, a more soluble (partially acetylated) form of the polysaccharide.^[94,95] Chitosan and protein composite films that mimic the chemical composition and phase-separated laminar arrangement observed in the cuticle of arthropods have been fabricated using casting methods.^[94] In this work, the protein used was insoluble fibroin. The composite films, referred to as “shrilk” (chitosan derived from shrimp shells combined with silk fibroin), displayed high strength and toughness in a low density and light-weight material (Figure 15A).^[94] Mechanical testing of films revealed a strength twice that of chitosan (the composite’s strongest component), as well as increased fracture toughness.^[94] The properties of chitosan-fibroin mimics also displayed a significant dependence on hydration, similar to what is observed in the cuticle of crustaceans and insects.^[94] These biomimetic cuticle inspired materials have potential applications in packaging, as replacement for plastics, as they are environmentally friendly and biodegradable.^[94]

Chitin and/or chitosan obtained from crustacean waste can also be used in biomedical applications as chitin is biocompatible and has a low toxicity.^[96,97] Chitosan acetate films have been fabricated from chitosan obtained from shrimp. These films have shown the ability to increase healing of burns, wounds and ulcers, resulting in noticeable skin recovery in periods of 1–2 weeks (Figure 15B).^[96] Chitosan

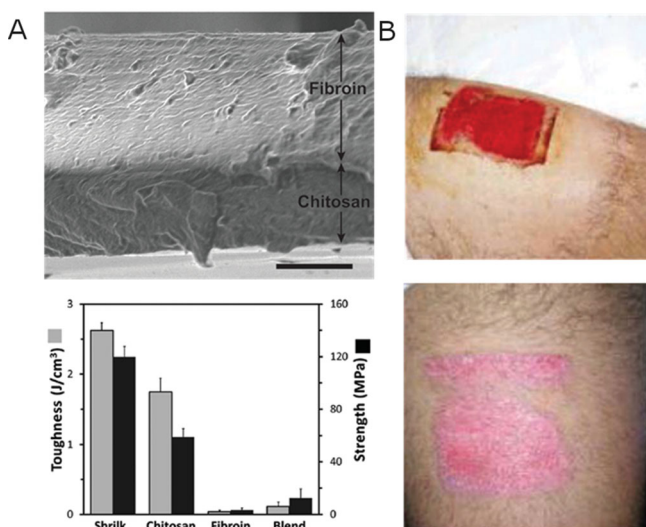


Figure 15. (A) Microstructure (scale bar is 2.3 cm) and mechanical properties of “shrilk” composites. Reproduced with permission.^[94] 2012, Wiley. (B) Chitin acetate films prepared using shrimp chitin used to promote healing after tattoo removal. Photographs show the wound following film placement, and the wound 14 days later. Reproduced with permission.^[96] Copyright 2008, Springer.

helps to speed recovery and prevent infection and fluid loss in patients with skin damage.^[96] Additionally, the material is biodegradable by the human body, eliminating the need for surgical removal of the film following treatment.^[96] Chitin nanofibrils can be produced from crustacean waste, by a patented process of isolating chitin nanocrystals.^[97] These needle-like fibrils, with dimensions on the order of $240 \times 5 \times 7$ nm, have potential applications in biomedical products and biomimetic cosmetics. Nanostructured chitin displays molecular signaling activity at a cellular level, thus chitin nanofibrils can be used to improve the cellular metabolism of the skin.^[97] A thorough review on biomedical applications of composites containing chitin and chitosan was presented by Khor and Lim.^[98] Chitin and chitosan waste is readily available (via fisheries), and the reuse of this waste contributes to a sustainable environment.

Beyond the native chitin and chitosan used as biomimetic scaffolds, additional features enhance the toughening and strengthening of biological composites. The versatility of properties observed in the cuticle is increased, for example, by the degree of tanning (cross-linking) of the protein, which increases the rigidity of the structure.^[62] This sclerotization process is most often discussed in insects, as mineralization plays a larger role in the hardening of the crustacean cuticle. Protein stabilization, however, does take place in the crustacean exoskeleton, likely through quinone-tanning or the presence of di- and tri-tyrosine amino acids.^[54] Tanning of proteins by the oxidation of catecols occurs in nature to provide stiffness and mechanical stability.^[99] To examine the role of tanning in the cuticle, composite mimics have been fabricated using cellulose paper as a framework for the deposition and tanning of proteins.^[99] Tanned composites display increased stiffness and hydrophobicity, providing a model system for the understanding of the tanning process in the

cuticle.^[99] Synthetic mimics of the non-mineralized membranous layer of the crustacean cuticle have also been fabricated, with potential applications in food packaging and biomaterials.^[100]

The pore canals present in the crustacean cuticle provide a combination of toughness and stiffness, while maintaining low weight.^[62] Chitin matrices with directional porosity and defined pore size have been synthesized using chitin gels loaded with specific concentrations of calcium carbonate.^[95] The calcium carbonate in the gel reacts with hydrochloric acid, producing carbon dioxide gas which creates the pore structure.^[95] The concentration of calcium carbonate, therefore, can be chosen to tune properties such as pore size and total porosity, and thus control mechanical properties.^[95] Another approach to the fabrication of porous chitin matrices is freezing and subsequent lyophilization of chitin gels.^[101] This approach can be used to synthesize materials with smaller pore diameter (minimum 10 μ m), where porosity is controlled by the freezing temperature and chitin gel density.^[101] Porous chitin matrices show water and vapor permeability, as well as the ability to absorb water.^[95,101] Porous chitin scaffolds have also been mineralized with hydroxyapatite to produce a composite *in situ*.^[102] Such materials have potential utility in medical applications including drug delivery systems, tissue engineering, and, for the case of hydroxyapatite mineralization, bone implants.^[30,95,101,102] A review of biomimetic mineralization on chitin and chitosan was presented by Falini and Fermani.^[103]

Experiments on mineralization of calcium carbonate in the presence of chitin (or chitosan) have explored the ability of the organic scaffold found in the cuticle to control phase and orientation of mineral in the laboratory.^[104] Thin film coatings of CaCO_3 , consisting of calcite and vaterite, have been prepared on chitin fibers in the presence of the acid rich polymers poly(acrylic acid), poly(L-aspartate) and poly(L-glutamate).^[105] Without the addition of these additives, characteristic rhombohedral calcite crystals form on chitin, which shows that the chitin fibers themselves do not influence crystallization, but that in the presence of acid-rich polymers, phase and morphology are altered.^[105] Biomimetic mineralization of supersaturated solutions of calcium carbonate has also been carried out using chitosan film as a substrate, and various concentrations of poly(acrylic acid) as an additive.^[106,107] Here the poly(acrylic acid), PAA, concentration was modified to control nucleation, growth and morphology of crystals. The addition of PAA results in protonated nitrogen and carboxylate anions on the film surface, thus initiating nucleation from these surface charged sites.^[106,107] PAA in this work was shown to promote heterogeneous nucleation and inhibit homogenous nucleation.^[106] Aragonite thin films have been prepared *in vitro* on chitosan matrices, utilizing poly(aspartate) (pAsp) and magnesium additives.^[108] Again, in the absence of additives, rhombohedral calcite crystals were formed on chitosan, indicating that the chitosan itself does not alter crystal morphology.^[108] The introduction of pAsp, however, led to the formation of thin films with homogeneous thickness, while the addition of MgCl_2 resulted in selective deposition of aragonite and a smoother film surface.^[108] These studies emphasize the importance of additives

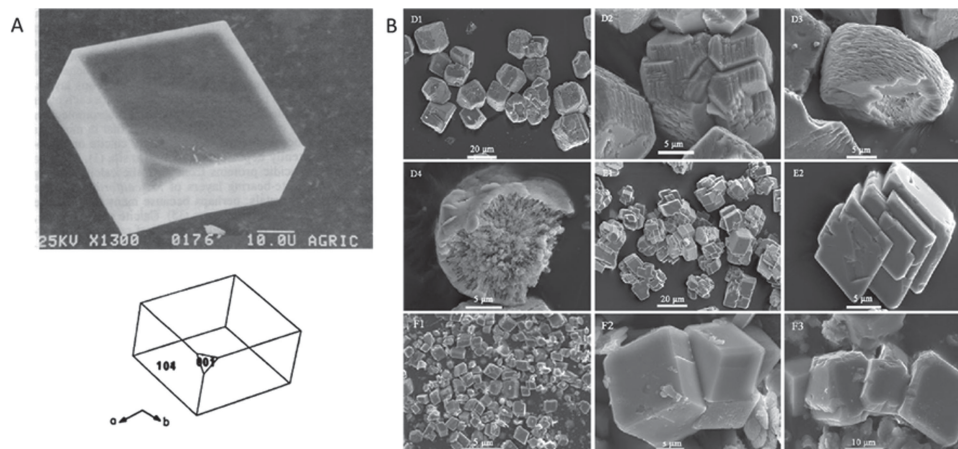


Figure 16. (A) Calcite crystal nucleated on a surface containing acidic proteins. The small (001) face was attached to the vial surface. Reproduced with permission.^[109] 1985, National Academy of Sciences. (B) Calcium carbonate crystals grown in the presence of various biological materials. The D group is microbial carbonic anhydrase, the E group is bovine carbonic anhydrase and the F group is water (control). Reproduced with permission.^[111] Copyright 2010, Elsevier.

in the biomineralization process, which will be discussed further in the following section.

4.3.2. Additives

In vitro Mineralization: The influence of various additives on crystallization has been examined *in vitro*. Such studies have shed light on the role of additives in crystal nucleation, growth and morphology. In solution, soluble acidic macromolecules, such as those found in the crustacean cuticle, inhibit crystallization, as they bind to growth sites over the entire crystal surface, preventing growth.^[71,109,110] In contrast, when associated with an insoluble template, the same macromolecules promote crystallization.^[71,110] This occurs because, when immobilized, the acidic macromolecules bind to only one surface of the crystal nucleus, allowing for growth from the other surfaces.^[109] Additives are also stereoselective, binding preferentially to certain crystal faces, and thus influencing growth rate and morphology.^[109] This fact was shown in a study which isolated acidic matrix proteins from calcitic and aragonitic layers of a bivalve shell.^[109] When calcite crystals were grown in solution with the aspartic acid-rich proteins, not only was a characteristic rhombohedral shape observed, but crystals also developed a small (001) face at one vertex. When grown on glass or plastic surfaces previously incubated with protein solutions, the calcite crystals grew with their (001) face in contact with the surface (**Figure 16A**). The (001) plane of the calcite crystal is the plane along which carbonate ions are aligned, making it the optimal plane for interaction with a calcium-loaded aspartic-acid rich protein.^[109]

The changes in cuticular proteins that trigger mineralization of the new exoskeleton following a molt have been used as inspiration for controlling the nucleation time and morphology of calcium carbonate in solution.^[69] For this study, cuticular proteins extracted from crabs at various times after molt were added to solutions of artificial seawater with CaCl_2 and NaHCO_3 added to initiate mineralization.^[69] The pH of the solution was measured as an indicator of crystal nucleation time. Cuticle extracts, as well as commercially obtained

acidic macromolecules of polyaspartate and polyglutamate, increased the time to nucleation of CaCO_3 versus control samples.^[69] In another approach to examining the effect of cuticular proteins (pre and post-molt), sample coupons of crab carapace from various stages in the molt cycle were used as a mineralization template.^[110] Decalcified coupons of crab cuticle were suspended in crystallization solution, and the time to crystal nucleation was again monitored through pH change. Cuticle samples showed a shortened induction period (time prior to nucleation) in post-ecdysial vs. pre-ecdysial samples (2.5 min vs. 15.3 min).^[110] It is suggested that this behavior relates to the greater fraction of unbound protein in the pre-molt cuticle, which inhibits crystallization.^[110] Consistent with previous studies, coupons of chitin alone, which do not contain proteins, were not found to promote crystallization^[110] while chitosan complexed with synthetic peptides promoted crystallization.^[110] Lastly, soluble matrix isolated from the crab carapace was shown to inhibit crystallization in solution.^[110]

An additive known to be important for the mineralization process following ecdysis is the enzyme carbonic anhydrase. Carbonic anhydrase is thought to catalyze the production of carbonate ions, mobilize calcium carbonate, and help to lay down new mineral layers.^[24,73] It is found with maximum activity during the calcification stage, immediately following a molt.^[24] The influence of microbial carbonic anhydrase on calcium carbonate precipitation has been studied *in vitro*.^[111] In one study, carbonic anhydrase was shown to increase the precipitation rate of calcium carbonate over control samples and other biological factors including carboxymethyl chitosan and glutamic acid.^[111] The morphology of crystals obtained in the presence of different additives varied significantly, with carbonic anhydrase use resulting in cubic and polyhedral morphologies (**Figure 16B**).^[111]

The presence of different matrix molecules (specifically proteins) is linked to different polymorphs of calcium carbonate.^[9] To investigate the influence of specific additives on mineral phase, an *in vitro* study was performed using soluble

macromolecules from an organism containing both ACC and calcite in different regions (spicules from the calcareous sponge *Clathrina*).^[66] Analysis of each region revealed proteins rich in glutamic acid and/or glutamine, serine, glycine and polysaccharides in the amorphous region, while proteins rich in aspartic acid and asparagine (no polysaccharides) were found in the calcitic region. This is a commonly reported theme in biological composites; glutamic acid is associated with the formation of an amorphous phase, and aspartic acid is found with crystalline mineral.^[45] For example, proteins extracted from a gastrolith, which contains only ACC, have been sequenced and shown to be rich in glutamic acid and glutamine.^[71] When small amounts (1.0 µg/ml) of amorphous region macromolecules extracted from *Clathrina* were added to saturated solutions of CaCO₃, stable amorphous phases were formed.^[66] This suggests that the polysaccharides and proteins in the amorphous region help to form and stabilize the amorphous phase. The additions of macromolecules from the calcitic region, in contrast, resulted in the growth of calcite crystals, with a modulation of crystal growth in the direction of the c-axis.^[66]

The role of amorphous mineral as a transient phase has also been examined *in vitro*. Studies have shown that an amorphous calcium carbonate precursor phase, created through the addition of an acidic polypeptide (polyaspartate), can be utilized to form CaCO₃ thin films, as well as unusual morphologies such as spiral pits and helical protrusions.^[67,112] The addition of polymers in this process results in sequestration and concentration of calcium ions and delays crystal nucleation and growth, leading to crystalline products which retain the shape of the precursor droplet and display nonequilibrium crystal morphologies.^[67] This is analogous to the role of macromolecules in biological mineralization processes and is attractive from a biomimetic standpoint as it is an environmentally benign process, carried out in an aqueous environment at room temperature.^[67] Addition of magnesium in this process was shown to decrease the amount of polymer necessary to form the precursor phase and increase the amorphous to crystalline transition rate.^[113] Helicoidal crystals of vaterite have also been reported with the addition of poly α,β-aspartate.^[114] Additionally, template-directed biomimetic deposition and crystallization of amorphous calcium carbonate has been used to produce millimeter sized single calcite crystals with controlled shape and orientation.^[115]

The influence of other soluble biological and synthetic molecules (including acidic polysaccharides), inorganic phosphate, and organic phosphorus-containing oxyanions, on calcium carbonate crystallization has also been examined.^[116] These additives, introduced at room temperature in aqueous solution, influence the phase, morphology and texture of calcium carbonate.^[116] The additive orthophosphate, for example, was shown to be a strong inhibitor of crystallization, with high concentrations resulting in an amorphous calcium phosphate precipitate.^[116] The use of sodium triphosphate as an inhibitor to crystallization has also been reported, with increasing concentration resulting in an increase in time prior to crystallization, followed by the precipitation of a calcium carbonate hexahydrate phase.^[117] The presence of phosphate ions has also been observed to stabilize amorphous biogenic

mineral, with stability increasing as a function of phosphate content.^[118] This is consistent with observations of phosphate in amorphous regions of the lobster cuticle, where it has been hypothesized that amorphous calcium carbonate and amorphous calcium phosphate exist not as two separate phases, but are combined at the molecular level as a calcium carbonate/phosphate phase.^[43] The use of various polymers as a form of surfactant and stabilizer has also been reported.^[45] This important class of additives can influence crystallization in several ways. Phosphoserine, in particular, is thought to be important in polymer-crystal interactions.^[45]

Proteins, as discussed, are also critical to biomineralization. While much work remains in the effort to sequence and understand crustacean cuticular proteins, some insight into the role of these macromolecules has been obtained. The well-known Rebers-Riddiford domain, found in many cuticle proteins, is believed to lead to chitin-binding, and is involved in the formation of the organic network used to template mineral growth.^[9] An 18-residue domain referred to as cuticle_1, is found only in the hard cuticle of crustaceans, and is thought to play a role in calcite crystal growth.^[9,119] Other proteins are important for *in vivo* calcium precipitation,^[9] binding of mineral to organic, and stabilizing the structure of chitin fibers.^[30] Studies have been published on characterization of proteins from the lobster *Homarus americanus*^[120,121] and the crab *Cancer pagurus*.^[119]

Magnesium and Water: Stabilization of the Amorphous Phase: While crustaceans occasionally utilize crystalline mineral for strength and stiffness, the bulk of the cuticle is composed of amorphous mineral. In fact, crustaceans are one of the most prevalent producers of ACC in the animal kingdom.^[71] There are several benefits to an amorphous phase as the matrix of these biological composites. Amorphous mineral, unlike a crystalline material, is isotropic and can sustain mechanical loads in all directions.^[45,66,68,71,72] Additionally, calcium storage in the form of ACC enables calcium mobility following a molt^[9,73]. This aids in decalcification of the cuticle prior to molt, as well as repair of the cuticle during the intermolt stage.^[9] Lastly, by depositing mineral in an amorphous phase, the organism can form mineralized parts with any desired shape.^[45,65] This has been demonstrated in a study where an ACC precursor was used to form calcite crystals within a porous membrane. The crystalline material was shown to take on the cylindrical shape of the 3 µm diameter pores, indicating that an amorphous phase can be utilized to produce a crystalline material with morphological features imposed by their environment.^[122] While macromolecules such as glutamic acid and glutamine play a role in stabilizing amorphous mineral in the crustacean cuticle, two other additives are critical to this function: magnesium and water.

Magnesium is often found in the cuticle, and is typically associated with amorphous mineral, or found as Mg-calcite. Magnesium is present in high concentrations in seawater (50–60 mM, approximately 5 times more abundant than Ca), and is known to have an inhibitory effect on calcite formation.^[76,118] Mg K-edge X-ray absorption spectroscopy investigations have revealed a shortened Mg-O bond length in amorphous mineral phases, indicating a lower coordination

number, and/or the presence of water molecules in the first coordination sphere, with both cases resulting in constraints on the system and therefore stability.^[118] Calcium carbonate precipitates formed from solutions with a magnesium to calcium ratio greater than or equal to four yield a precursor amorphous phase even in the absence of additional additives.^[123] This is attributed to the fact that the presence of magnesium ions leads to an increase in the degree of supersaturation of the solution, resulting in the precipitation of amorphous particles.^[123] Additionally, magnesium ions substitute into Ca lattice positions inhibiting calcite crystallization at Mg/Ca ratios greater than 4.^[118]

The addition of magnesium in aqueous solutions has been reported to result in longer times for precipitate formation, and lower quantities of product, with increasing Mg content.^[124] At all concentrations of Mg studied, amorphous calcium carbonate was the first phase to form, with the stability of the amorphous phase increasing with Mg content.^[124] An amorphous precursor with 8 mol% Mg was stable for under 30 minutes, while a precursor containing 24 mol% Mg was stable for up to 14 hours.^[124] Eventual crystallization resulted in a range of phases directly related to the Mg content.^[124] Counterintuitively, the addition of too large a quantity of Mg (9:1 ratio Mg:Ca) has been shown to reduce the stability when compared to ratios of 4:1 or 2:1.^[77] In this case, a nesquehonite phase forms rather than the kinetically-inhibited magnesian calcite phase.^[77] The addition of organic molecules, specifically carboxylated organic acids, have been shown to increase the ratio of Mg/Ca in ACC over that which is attainable in the absence of additives,^[125] providing further insight into biological mineralization methods. Magnesium has also been shown to stabilize amorphous calcium phosphate, with the direct addition of dissolved phosphate into seawater resulting in stable amorphous calcium phosphate, and the addition of phosphate into Mg-free artificial seawater or distilled water resulting in the immediate precipitation of apatite.^[126] Controlled experiments have also examined the kinetics of transformation from ACP to apatite at various Mg/Ca molar ratios, with more Mg resulting in a slower transformation.^[127]

Following the molt process in crustaceans, amorphous mineral is transported through pore canals to designated areas of the cuticle and crystallized in specific regions. Amazingly, the organism is capable of specifically controlling the stability of the amorphous phase and the crystallization process. For this to occur, crystallization must be deliberately inhibited, as transformation to the crystalline phase is not only thermodynamically favored, but also kinetically fast.^[65] Crystallization of magnesium stabilized precursors has been shown to be associated with proteins rich in aspartic acid.^[128] This finding indicates that magnesium and Asp-rich proteins act in tandem as a crystallization switch during the biomineralization process.^[128] The Asp monomer alone acts to stabilize the amorphous phase in solution. However, when introduced to the magnesium stabilized amorphous phase, Asp triggers mineralization. Thus, in the biological system, magnesium stabilizes the amorphous phase (acting as the “off” switch) while the Asp monomer reduces the stability of the system (switches mineralization “on”), resulting in a

phase transformation to calcite or hydroxyapatite.^[128] This biological switching mechanism, which has been successfully replicated in *in vitro* mineralization experiments for both calcium carbonate and calcium phosphate,^[128] can be implemented in biomimetic systems to intelligently control material fabrication.

Two types of amorphous calcium carbonate are reported in the crustacean cuticle. Occasionally, ACC is formed as a precursor phase to a crystalline calcium carbonate.^[72,76,129] In biological structures, this transient phase is not hydrated, containing no water molecules in its lattice structure.^[71,129] In addition to transient precursor phases, stable forms of amorphous calcium carbonate are commonly found in the cuticle. These stable forms of biological ACC are hydrated, with one mole of water reported per mole of calcium carbonate.^[71,72] Thermogravimetric analysis (TGA) of biological samples of stable amorphous calcium carbonate show significant water loss, of approximately 15% by weight, compatible with the 1:1 stoichiometry.^[73,130] TGA has also been performed on amorphous calcium carbonate phases prepared with and without the addition of additives such as magnesium.^[131] Weight loss curves and complementary differential scanning calorimetry (DSC) data from these samples reveal that regardless of additives, all samples contain a similar water content (7 wt%), and that with the loss of structural water (from 100–250°C) a transformation to calcite is initiated.^[131] This influence of hydration on the stability of the amorphous phase is consistent with TGA/DSC results from other studies.^[132,133] The existence of bound water in amorphous calcium carbonate has also been observed using IR,^[134,135] which has shown a strong water signal in the amorphous material, decreasing through the crystalline polymorphs in order of stability (**Figure 17**).^[136] In a comprehensive study using TGA, DSC and IR to track dehydration and crystallization of synthetic ACC and transient biogenic ACC to Calcite it was shown that the dehydration of ACC to an anhydrous amorphous phase is an irreversible process that precedes crystallization.^[137] These results suggest that, in addition to other additives, hydration is critical to the stability of amorphous mineral.

The ability of water to stabilize an otherwise unfavorable mineral phase in biological systems has also been observed in bone, which displays a carbonated apatite structure with a much lower degree of crystallinity than synthetic carbonate apatite.^[138] In this case, water molecules occupy vacancies in the crystal lattice, stabilizing the structure via hydrogen bonding and preventing transformation to a more crystalline and thermodynamically stable phase.^[138] While no crystal lattice is present in amorphous calcium carbonate, a similar mechanism may be at work. In fact, nuclear magnetic resonance (NMR) analysis of ACC synthesized without the addition of any additives has shown that a significant portion of the hydrogen-bearing species in ACC are present as structural water, which is assumed to be coordinated to Ca ions, suggesting that hydrogen bonding plays a critical role in the stabilization of the amorphous mineral.^[134]

More insight into the stabilization of amorphous calcium carbonate has been obtained through computer simulations. The thermodynamics of ACC have been explored at

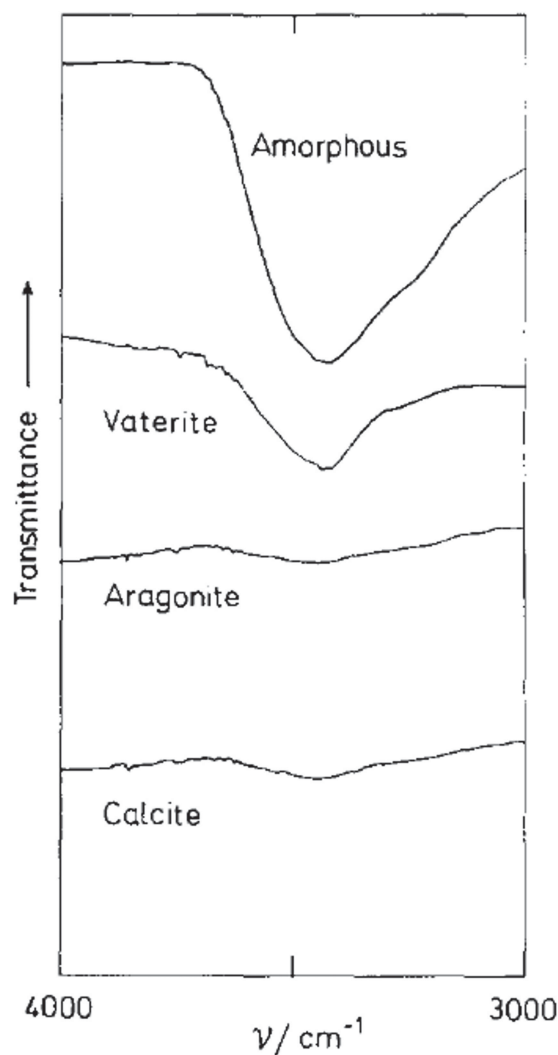


Figure 17. IR absorption bands in the region from 3000 to 4000 cm^{-1} for amorphous calcium carbonate, vaterite, aragonite, and calcite. Amorphous calcium carbonate shows an absorption band at 3430 cm^{-1} and a shoulder at 3220 cm^{-1} , characteristic of O-H bonds, indicating water content. Reproduced with permission.^[136] Copyright 1989, Elsevier.

an atomistic scale through force field simulations.^[139] Examining the enthalpy of amorphous calcium carbonate particles of various size as a function of water content, it has been shown that the enthalpy of the system decreases as the incorporation of water into the structure increases, indicating the ability of water to stabilize the system.^[139] Additionally, the thermodynamically favored stoichiometry of hydrated ACC has been shown to be dependent on size of individual ACC particles, with more water required for larger particle size.^[139] A reverse Monte Carlo method has also been utilized to model hydrated ACC at an atomistic scale, revealing a nanoporous structure consisting of a calcium rich framework containing a hydrogen bound carbonate/water component within approximately 1 nm sized open channels.^[75] It is suggested that this design leads to stabilization of the amorphous phase, with a conversion to a crystalline structure requiring expulsion of the water from the coordinated carbonate/water

component in the open channels, and subsequent incorporation of the remaining calcium into the framework.^[75] The porous structure also allows for the incorporation of additives to further stabilize the amorphous phase.^[75] Interestingly, Mg has a higher energy barrier to dehydration than Ca, potentially indicating the cooperation of Mg and water in the stabilization of the amorphous phase.^[118] This hypothesis is bolstered by data showing that the presence of Mg promotes ACC hydration.^[140]

4.3.3. Polymer Templates

Beyond the use of additives to control mineralization, another common approach to biomimetic synthesis of organic-inorganic composites is the use of polymers to template mineralization. These synthetic organic templates include Langmuir monolayers, self-assembled monolayers (SAMs), and block copolymers. A large body of literature exists on this topic, and we will present only a small portion of it here, focusing on studies with direct relevance to the crustacean cuticle. For more information on the topic the reader is directed to the following review papers: An early review on biomimetic mineralization of nano-scale particles using polymer templates, specifically Langmuir monolayers and Langmuir-Blodgett films, was presented by Calvert and Rieke.^[90] Efforts to grow CaCO_3 on protein-derivatized substrates and other synthetic surfaces are also presented in this work.^[90] A comprehensive review on biomimetic synthesis of organic-inorganic composites, specifically calcium carbonate nucleation and growth on synthetic substrates (including Langmuir monolayers and SAMs) were presented by Naka and Chujo.^[141] This review also contains details of *in vitro* mineralization experiments, nucleating calcium carbonate in the presence of proteins extracted from mollusk shells, as well as the influence of low-molecular-weight organic additives and double-hydrophilic block copolymers on crystallization.^[141] A review article by Sanchez et al. provides details on advances in polymer science and inorganic chemistry for the production of hybrid organic/inorganic materials with complex hierarchical structures.^[23] Finally, Li and Kaplan have presented a review on molecular scale organic-inorganic composite mimics, focusing on the mineralization of hydroxyapatite, silica and calcium carbonate.^[142]

Initial work by Mann and coworkers examined the biomimetic crystallization of supersaturated calcium carbonate solutions on compressed Langmuir monolayers.^[143,144] In the absence of a monolayer, rhombohedral calcite crystals were formed. With a structured organic template, however, oriented calcite, aragonite and vaterite were obtained, with phase and morphology dependent on experimental conditions. The degree of compression of the film, the surfactant and head groups used, and the addition of additives influenced the rate of nucleation as well as the phase and morphology of the crystals. With compressed monolayers of n-icosyl sulfate and n-icosyl phosphate, calcite crystals nucleated preferentially on the (001) face, and aragonite was nucleated when Mg was introduced as an additive (**Figure 18A**).^[143] The first *in-situ* observation of nucleation and growth of an amorphous mineral film on a Langmuir monolayer was reported by DiMasi et al.^[145] In this work, a

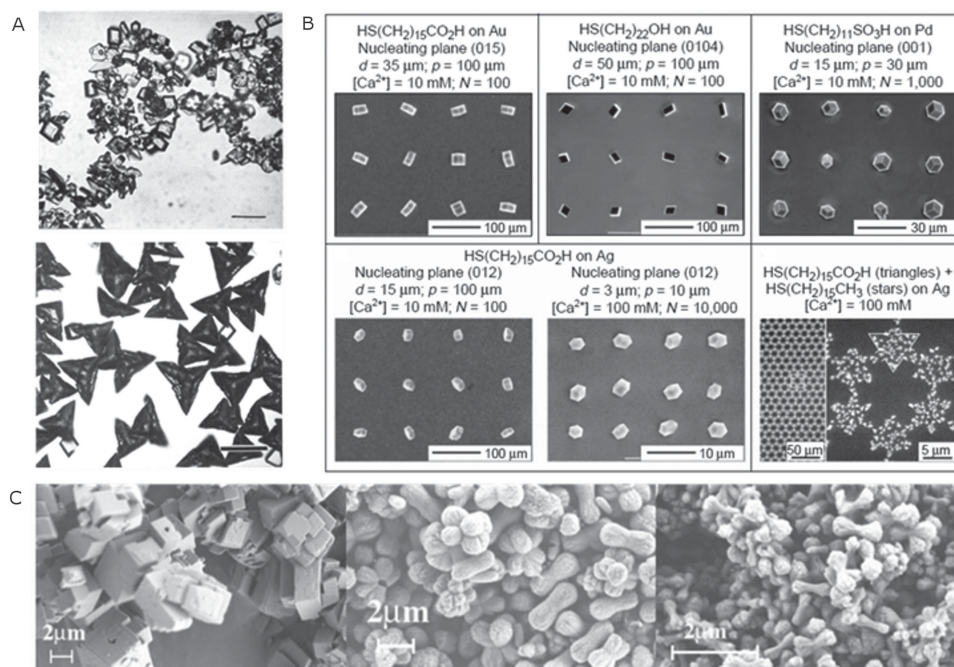


Figure 18. (A) Calcite crystals grown in the absence of a monolayer (top) and calcite crystals formed under a compressed monolayer of n-eicosyl sulfate (bottom) scale bars 50 μm . Reproduced with permission.^[143] Copyright 1994, ACS Publications. (B) Ordered arrays of calcite crystals formed on micropatterned self-assembled monolayers. Reproduced with permission.^[146] 1999, Nature. (C) From left to right: calcium carbonate nucleated without the presence of polymer, calcium carbonate nucleated in the presence of the double-hydrophilic block copolymer poly(ethylen glycol)-block-poly(methacrylic acid) with a polymer to CaCO_3 ratio of 0.3, and calcium carbonate nucleated with a polymer to CaCO_3 ratio of 0.9. Reproduced with permission.^[151] Copyright 2004, AIP Publishing.

dilute poly(acrylic acid) additive was utilized to mimic the soluble macromolecules found in biological systems resulting in the formation of a hydrated amorphous film.^[145] Synchrotron X-ray scattering was utilized to provide real-time measurements on an atomic length scale, monitoring the growth of the calcium carbonate mineral from a collection of cations at the monolayer interface, to a macroscopic hydrated film.^[145]

While calcium carbonate nucleation on Langmuir monolayers has offered insights into the control of crystal phase and orientation, it is an oversimplified case when modeling biomimetalization.^[45] A more complex polymer surface for biomimetic mineralization studies can be provided by self-assembled monolayers (SAMs). Nucleation of periodic arrays of calcium carbonate has been demonstrated on micropatterned SAMs, resulting in controlled location, density, phase, size and orientation of crystals (Figure 18B).^[146,147] Growth of calcite on six different crystallographic planes has been achieved using patterned alkanethiols on metal substrates of gold and silver.^[147] The more ordered structure of functionalized SAMs results in an organic surface with greater control and selectivity than Langmuir monolayers, with crystal properties dictated by functional group and support material properties.^[146,147] Hydroxyl-terminated SAMs have also been used as a template for synthesis of a stable amorphous precursor phase, where controlled crystallization (orientation, location and pattern) can be triggered through the introduction of a second carboxylic-acid terminated SAM template.^[74]

A different route to polymer controlled mineralization is the use of block copolymers as an organic template. Using block copolymers, the first example of a single reaction system capable of nucleating and growing any calcium carbonate polymorph from an amorphous precursor phase was achieved.^[148] In this work, the addition of a single additive, poly(sodium 4-styrene sulfonate-co-N-isopropylacrylamide), was shown to exert control over calcium carbonate mineral formation, resulting in calcite, aragonite or vaterite formation dependent on concentration variations of calcium and polymer ions.^[148] An amphiphilic molecule shows affinity for multiple substrates. This means it has the ability to simultaneously bind to two material types (e.g., the mineral and chitin found in the crustacean cuticle).^[45] Amphiphilic block copolymers, specifically double-hydrophilic block copolymers, consist of two water-soluble blocks of different chemical composition. One block is designed to interact with inorganic minerals, while the other block promotes solubilization in water.^[45,149–151] This class of block copolymer can be used to template mineral growth in aqueous solution at room temperature, in much the same way that proteins and polysaccharides control mineralization in biological systems. For this reason, these polymer templates have been utilized in the biomimetic control and stabilization of mineralization.^[152,153]

A double-hydrophilic block copolymer with a poly(acrylic acid) block, drawing inspiration from the acidic proteins identified in biological samples containing stable ACC, was used to stabilize nanosized amorphous calcium

carbonate against coalescence in solution.^[154] Block copolymers, with one block functionalized with polyelectrolyte additives such as poly(methacrylic acid), polyaspartic acid, phosphonate and poly(ethylenimine)-poly(acetic acid), have been used to precipitate calcium carbonate with controlled crystal phase, size, and shape from an aqueous solution (figure 18C).^[149,151] Similar results have been obtained with calcium phosphate, using a copolymer with one poly(ethylene oxide) block and one poly(methacrylic acid) block, using pH to control morphology, phase, and crystallization kinetics in the formation of organic/inorganic hybrid structures.^[150] In an extension of these studies, double-hydrophilic graft copolymers, with tunable properties such as main chain length and ionic group content, and number and size of side chains, have also been utilized as additives in the crystallization of CaCO₃.^[155] These graft copolymers, consisting of a polyacetal backbone modified with carboxylate and poly(oxyethylene) side chains, were used to template mineralization, resulting in controlled crystal size and shape.^[155] Biomimetic nanostructured ceramic materials prepared in this way have potential applications in a range of technological applications.

While the bulk of this discussion has focused on calcium carbonate mineralization, calcium phosphate is also observed in specialized regions of the crustacean cuticle.^[12,16,19,44] Phosphorus is generally associated with protective functions, as discussed in the case of the American lobster.^[12,44] In the stomatopod dactyl club, the outer impact region, which makes up the hardest portion of the cuticle, is composed of hydroxyapatite.^[19] A review by Oliveira et al. has been presented that covers advances in biomimetic calcium phosphate coatings.^[64] The reader may also find interest in other biomimetic studies inspired by bone and/or the nacreous layer of mollusk shells.^[156–158]

4.4. Biomimetic Composites From Synthetic Materials: Nanoscale and Beyond

Biomimetic composites inspired by the crustacean cuticle have not only been fabricated using organic and mineral phases, but also high performance composite components; specifically fiber reinforced plastics and layered structures. While there is value in understanding and replicating the biomineralization process using materials such as calcium carbonate, nature is limited in its selection of materials. Engineers and materials scientists have at their disposal a wider range of material choices. Translating design strategies observed in nature to synthetic materials can result in composites with altered properties. In this subset of the field of biomimetics, the end goal is to fabricate nature-inspired structures, architectures, and interfacial designs, leaving behind the biological constraints of keeping an organism alive.^[22,142] Such biomimetic composites have potential uses in armor, aerospace, and automotive applications, where light-weight structures with high strength and toughness are required.

In studies combining both natural and synthetic materials, nanocomposites have been fabricated using chitin

whiskers as an environmentally friendly reinforcing phase in matrices of various thermoplastic and natural materials.^[159–163] Crystalline fragments of chitin with lengths of 50–300 nm (average 150 nm) and diameters of 10 nm (aspect ratio approximately 15) were embedded in thin films of latex to form a nanocomposite.^[159] Above the glass transition temperature (T_g) of the matrix, an increase in the composite modulus was observed as a function of increasing chitin content.^[159] Chitin whiskers have also been used to reinforce soy protein isolate (SPI) plastics to form biodegradable nanocomposites.^[160] Here, chitin whiskers with lengths of 500 ± 50 nm and diameters of 50 ± 10 nm were incorporated into an SPI matrix.^[160] Again, an increase in storage modulus was observed at temperatures exceeding T_g , and a decrease in water uptake was reported as a function of chitin whisker content.^[160] Tensile strength and Young's modulus also increased with increasing chitin loading, up to a critical chitin content of 20 wt%.^[160] In a series of experiments, Nair and Dufresne utilized crab shell chitin whiskers as reinforcement in bionanocomposites of natural rubber.^[161–163] Whiskers with an average aspect ratio of 16 (length 240 nm, diameter 15 nm) were embedded in vulcanized and unvulcanized rubbers, using multiple manufacturing methods. Swelling behavior in toluene was shown to decrease with increasing chitin content, indicating a barrier to water absorption.^[161] Storage modulus and Young's modulus were shown to increase as a function of chitin content, with mechanical properties dependent on processing route.^[162] Finally, chemical modification of the chitin whiskers was examined, which resulted in an increase in the adhesion between the reinforcement and matrix, but a decrease in mechanical properties because of destruction of the three-dimensional network of chitin whiskers achieved in the unmodified samples.^[163] These studies show that incorporating chitin as a reinforcing phase in nanocomposites results in greater thermal stability and reduced moisture absorption.

Composites inspired by the crustacean cuticle have also been fabricated with fiber reinforced plastics. This is a natural choice, as the aligned chitin fibers observed in the cuticle are reminiscent of unidirectional fiber reinforced materials, and, much like a composite laminate, the cuticle is composed of stacked layers of these unidirectional sheets. In one example, the pore canal transport network in the crustacean cuticle provided inspiration for incorporating holes into structural composites.^[164] Laminates containing preformed holes were fabricated with unidirectional carbon fiber-epoxy,^[165] as well as woven glass fiber-epoxy layers.^[164] By draping fibers preimpregnated with a matrix material around cylindrical pins of various diameters and subsequently curing the resin, holes were introduced into composite panels, leaving the fibers around the holes continuous.^[164,165] Tensile properties of laminates with preformed holes showed dramatic improvement over laminates with drilled holes (**Figure 19A**), as the stress concentrations created by broken fibers were eliminated using a biomimetic approach featuring fiber continuity around the pore openings.^[164,165]

The majority of studies on biomimetic fiber reinforced composites focus on the fabrication and testing of laminates

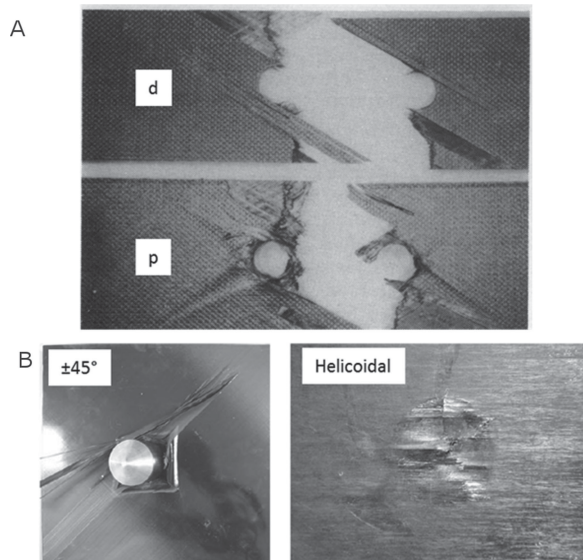


Figure 19. (A) Biomimetic fiber-reinforced composites (A) failure in a tensile test of an open-hole composite sample with a drilled hole (d) compared to a bio-inspired preformed hole. Reproduced with permission.^[165] 1993, Sage. (B) Impact damage in a composite sample with a $\pm 45^\circ$ layup compared to a helicoidal layup. Reproduced with permission.^[169] Copyright 2011, Dr. K. Ravi-Chandar.

with a helicoidal architecture, which draw inspiration from the rotated plywood motif observed in the arthropod cuticle. High performance composites have been fabricated with unidirectional fiber sheets in which each layer is rotated by a fixed angle from the layer below it to form a biomimetic Bouligand structure. Helicoidal composites formed from glass fiber-epoxy and carbon fiber-epoxy systems have been shown to exhibit increased pullout energy,^[166] fracture toughness,^[166–169] debonding resistance,^[167] and residual strength,^[168–170] over traditional composite layups. Another key benefit to a helicoidal design is an increase in impact resistance over traditional layups, resulting from crack redirection and prevention of damage propagation through the thickness of the structure (Figure 19B).^[167,170] These gains in material properties are a result of the gradual rotation angle between layers, which leads to a higher degree of isotropy, reduced interlaminar shear stresses, and crack deflection and resistance.^[167]

Another toughening feature observed in the crustacean cuticle is the layering of materials with different modulus for crack deflection. As detailed by Fratzl, crack propagation will be stopped in a layered material when the modulus ratio of the material on either side of an interface exceeds ≈ 5 , with no dependence on the relative thickness of each layer.^[171] This biological design strategy, incorporating layered structures with materials of differing modulus, has been reproduced with synthetic composites.^[172] Though largely inspired by bone and the nacreous layer of mollusk shells, these materials exhibit properties observed in the crustacean cuticle as well, notably in the incorporation of an ultra-hard exocuticle with a more compliant endocuticle. At the nanoscale, examples include layered composites of titanium dioxide (100 nm) and polyethylene (10 nm), which exhibit interpenetration at

the interface between layers, increased hardness, and a toughness four times that of monolithic TiO_2 .^[173] This increase in toughness arises from crack deflection at the interface between layers, as well as a reduction in crack propagation because of an elastic modulus mismatch.^[171,174] Also reported are zirconia composites with a thin (14 nm) organic interlayer, which display increased hardness and modulus over solution-deposited zirconia alone.^[175] At the macro-scale, for ballistic applications, armor materials have been developed with interlayers of varying modulus.^[176] Interlayers of rubber, Teflon and aluminum foam were inserted between an alumina ceramic tile strike face and a glass fiber-reinforced composite backing plate. The interlayers cause spreading and distribution of damage, in much the same way as the alternating stiff and compliant layers observed in the rotated plywood structure of the crustacean cuticle. The same principle is utilized in the fabrication of a class of materials referred to as micro-infiltrated macro-laminated composites (MIMLCs).^[177,178] These composite materials, fabricated through powder processing methods, consist of layers of a hard and brittle ceramic, interpenetrated at the micro-scale by thin layers of a soft phase with high ductility and toughness.^[177,178] During ballistic testing, cracks nucleated in the brittle phase were shown to be deflected at the interface with the ductile layer, resulting in high toughness.^[178] The production of such MIMLCs with a compositionally graded microstructure has also been demonstrated through solid-state processing methods.^[177]

At the global scale, the material and morphological features of the cuticle of the lobster *Homarus americanus* have provided design inspiration for the ICD/ITKE Research Pavillion 2012 (Figure 20).^[179] This structure represents a multidisciplinary effort combining engineering, architecture and biology. The pavilion, built in collaboration by the Institute for Computational Design (ICD) and the Institute of Building Structures and Structural Design (ITKE) at the University of Stuttgart, and biologists from the University of Tübingen, is a biomimetic structure composed of resin saturated glass and carbon fibers. To construct the pavilion, fibers were laid on a temporary frame using an automated process.^[179] After the resin was cured, this frame was removed, resulting in a free-standing structure. Fiber-optic sensors were integrated into the pavilion to continuously monitor stress and strain variations.^[179] Key design aspects inspired by the crustacean cuticle include the fibrous morphology and deliberate anisotropy of the structure. The fiber orientation is locally adapted and optimized based on loading conditions to allow for a minimum amount of material and maximum structural stiffness. The optimal fiber orientation in each region of the structure was determined through computer simulations and, as is observed in the crustacean cuticle itself, includes a helicoidal architecture where isotropic response is required, as well as unidirectional regions to accommodate directional loading. The thickness of the pavilion is only 4 mm, but the structure spans 8 m, yielding an efficient and lightweight structure.^[179] The pavilion is also hierarchical in nature, with glass fibers used for spatial partitioning, and carbon fibers contributing to load transfer and stiffness.^[179] This biomimetic design shows the potential for



Figure 20. (A) The completed ICD/ITKE Research Pavilion, along with architectural designs incorporating (B) a heliocidal structure for isotropic response and (C) unidirectional fibers for anisotropic loading. Reproduced with permission.^[179] Copyright 2012, ICD-ITKE.

a new paradigm in composite construction and architecture, drawing design strategies from millions of years of evolutionary structural optimization.

While interesting composite materials and structures have been achieved through inspiration from the crustacean cuticle, areas remain for continued research. As pointed out by several authors, a rich ground for the expansion of biomimetic composites lies in an improved understanding of the interface between the organic and inorganic phases.^[22,63,142] The properties of hybrid materials depend not only on the properties of each individual constituent, but also the synergy between them.^[180] Additional information is also needed for a better understanding of the function of cuticular proteins.^[46] In addition to mineralization, investigation of the degree of protein cross-linking, chitin-protein and protein-protein interactions, as well as the compositions of proteins, is needed to further understand their influence on the mechanical properties of the cuticle.^[119] Additional work is required to elucidate the specific functions of the proteins that have been sequenced in the crustacean cuticle, such as chitin-binding (organization and control of the organic matrix), recruiting and nucleating of mineral, and the regulation or inhibition of pre-molt mineralization. Another potential avenue for biomimetic research

is greater insight into of the ability of crustaceans to elaborate and resorb mineral.

Acknowledgements

The authors gratefully acknowledge financial support from the Air Force Office of Scientific Research (AFOSR-FA9550-12-1-0245) and the National Science Foundation (DMR-0906770). Helpful discussions with Professor Pablo Zavattieri, Christopher Salinas, and Nick Yaraghi are also acknowledged.

- [1] M. A. Meyers, A. Y. M. Lin, Y. Seki, P.-Y. Chen, B. K. Kad, S. Bodde, *JOM* **2006**, 36.
- [2] J. Curry, *Science* **2005**, 309, 253.
- [3] H. Jiang, X. Liu, C. Lim, C. Hsu, *Appl. Phys. Lett.* **2005**, 86, 163901.
- [4] U. G. K. Wegst, M. F. Ashby, *Philos. Mag.* **2004**, 84, 2167.
- [5] J. Weaver, Q. Wang, A. Miserez, A. Tantuocci, R. Stromberg, K. Bozhilov, P. Maxwell, R. Nay, S. Heier, E. DiMasi, D. Kisailus, *Mater. Today* **2012**, 13, 42.

- [6] J. C. Dunlop, P. Fratzl, *Annu. Rev. Mater. Res.* **2010**, *40*, 1.
- [7] H. A. Lowenstam, S. Weiner, *On biomineralization*, Oxford University Press, New York **1989**.
- [8] H. Fabritius, C. Sachs, D. Raabe, S. Nikolov, M. Friak, J. Neugebauer, *Chitin in the exoskeletons of arthropoda: From ancient design to novel materials science*, (Eds: N. S. Gupta), Springer, Dordrecht **2011**.
- [9] G. Luquet, *ZooKeys* **2012**, *176*, 103.
- [10] S. T. Brennan, T. K. Lowenstein, J. Horita, *Geology* **2004**, *32*, 473.
- [11] H.-O. Fabritius, C. Sachs, P. Romano Triguero, D. Raabe, *Adv. Mater.* **2009**, *21*, 391.
- [12] J. G. Kunkel, W. Nagel, M. J. Jercinovic, *J. Shellfish Res.* **2012**, *31*, 515.
- [13] D. Raabe, P. Romano, C. Sachs, H. Fabritius, A. Al-Swalmih, S.-B. Yi, G. Servos, H. G. Hartwig, *Mater. Sci. Eng., A* **2006**, *421*, 143.
- [14] G. Panganiban, A. Sebring, L. Nagy, S. Carroll, *Science* **1995**, *270*, 1363.
- [15] M. K. Schulz, C. G. Alexander, *Mar. Freshwater Behav. Physiol.* **2001**, *34*, 181.
- [16] H.-O. Fabritius, E. S. Karsten, K. Balasundaram, S. Hild, K. Huemer, D. Raabe, *Z. Kristallogr. - Cryst. Mater.* **2012**, *227*, 766.
- [17] F. Bobelmann, P. Romano, H. Fabritius, D. Raabe, M. Epple, *Thermochim. Acta* **2007**, *463*, 65.
- [18] C. Sachs, H. Fabritius, D. Raabe, *J. Mater. Res.* **2006**, *21*, 1987.
- [19] J. C. Weaver, G. W. Milliron, A. Miserez, K. Evans-Lutterodt, S. Herrera, I. Gallana, W. J. Mershon, B. Swanson, P. Zavattieri, E. DiMasi, D. Kisailus, *Science* **2012**, *336*, 1275.
- [20] M. S. deVries, E. A. K. Murphy, S. N. Patek, *J. Exp. Biol.* **2012**, *215*, 4374.
- [21] M. S. Rosenberg, *Biol. J. Linn. Soc.* **2002**, *75*, 147.
- [22] G. Mayer, M. Sarikaya, *Exp. Mech.* **2002**, *42*, 395.
- [23] C. Sanchez, H. Arribart, M. Madeleine, G. Guille, *Nat. Mater.* **2005**, *4*, 277.
- [24] M.-M. Giraud-Guille, E. Belamie, G. Mosser, *Comptes rendus Palevol* **2004**, *3*, 503.
- [25] A. G. Richards, *The integument of arthropods*, University of Minnesota Press, Minneapolis **1951**
- [26] M. N. Horst, J. A. Freeman, *The crustacean integument: Morphology and biochemistry*, CRC Press, **1993**
- [27] M.-M. Giraud-Guille, *Curr. Opin. Solid State Mater. Sci.* **1998**, *3*, 221.
- [28] Y. Bouligand, *Tissue Cell* **1972**, *4*, 189.
- [29] D. Raabe, A. Al-Sawalmih, S. B. Yi, H. Fabritius, *Acta Biomater.* **2007**, *3*, 882.
- [30] P. Romano, H. Fabritius, D. Raabe, *Acta Biomater.* **2007**, *3*, 301.
- [31] A. Becker, A. Ziegler, M. Epple, *Dalton Trans.* **2005**, 1814.
- [32] J. L. Arias, M. S. Fernandez, *Mater. Charact.* **2003**, *50*, 189.
- [33] H. Nagasawa, *Prog. Mol. Subcell. Biol.* **2011**, *52*, 315.
- [34] J. R. A. Taylor, J. Hebrank, W. M. Kier, *J. Exp. Biol.* **2007**, *210*, 4272.
- [35] C. Sachs, H. Fabritius, D. Raabe, *J. Struct. Biol.* **2006**, *155*, 409.
- [36] *Biology of the lobster homarus amaericanus*, (Eds: J. R. Factor), Academic Press, San Diego **1995**.
- [37] C. Sachs, H. Fabritius, D. Raabe, *J. Struct. Biol.* **2008**, *161*, 120.
- [38] A. Al-Sawalmih, C. Li, S. Siegel, H. Fabritius, S. Yi, D. Raabe, P. Fratzl, O. Paris, *Adv. Funct. Mater.* **2008**, *18*, 3307.
- [39] D. Raabe, P. Romano, C. Sachs, A. Al-Sawalmih, H.-G. Brokmeier, S.-B. Yi, G. Servos, H. G. Hartwig, *J. Cryst. Growth* **2005**, *283*, 1.
- [40] S. Nikolov, H. Fabritius, M. Petrov, M. Friak, L. Lymperakis, C. Sachs, D. Raabe, J. Neugebauer, *J. Mech. Behav. Biomed. Mater.* **2011**, *4*, 129.
- [41] D. Raabe, C. Sachs, P. Romano, *Acta Mater.* **2005**, *53*, 4281.
- [42] L. Cheng, L. Wang, A. M. Karlsson, *J. Mater. Res.* **2008**, *23*, 2854.
- [43] A. Al-Sawalmih, C. Li, S. Siegel, P. Fratzl, O. Paris, *Adv. Mater.* **2009**, *21*, 4011.
- [44] J. G. Kunkel, M. J. Jercinovic, *Mar. Biol. Res.* **2013**, *9*, 27.
- [45] *Biomineralization. From nature to application.*, (Eds: A. Sigel, H. Sigel, R. Sigel), John Wiley & Sons, Ltd, West Sussex **2004**.
- [46] S. Nikolov, M. Petrov, L. Lymperakis, M. Friak, C. Sachs, H.-O. Fabritius, D. Raabe, J. Neugebauer, *Adv. Mater.* **2012**, *22*, 519.
- [47] C. Linnaeus, *Systema naturae per regna tria naturae, secundum classes, ordines, genera, species, cum characteribus, differentiis, synonymis, locis.*, (Eds: Holmiae: Impensis Direct, Laurentii Salvii), **1758**.
- [48] P. Drach, *Annales de l'Institut Océanographique* **1939**, *19*, 382.
- [49] T. Hegdahl, J. Silness, F. Gustavsen, *Zool. Scr.* **1977**, *6*, 89.
- [50] T. Hegdahl, F. Gustavsen, J. Silness, *Zool. Scr.* **1977**, *6*, 101.
- [51] T. Hegdahl, F. Gustavsen, J. Silness, *Zool. Scr.* **1977**, *6*, 215.
- [52] B. S. Welinder, *Comp. Biochem. Physiol.* **1974**, *779*.
- [53] B. S. Welinder, *Comp. Biochem. Physiol.* **1975**, *52A*, 659.
- [54] B. S. Welinder, P. Roepstorff, S. O. Andersen, *Comp. Biochem. Physiol.* **1976**, *53B*, 529.
- [55] S. Patek, R. Caldwell, *J. Exp. Biol.* **2005**, *208*, 3655.
- [56] S. Patek, W. Korff, R. Caldwell, *Nature* **2004**, *428*, 819.
- [57] M. Burrows, *Z. vergl. Physiol.* **1969**, *62*, 361.
- [58] J. Currey, A. Nash, W. Bonfield, *J. Mater. Sci.* **1982**, *17*, 1939.
- [59] R. L. Caldwell, H. Dingle, *Naturwissenschaften* **1975**, *62*, 214.
- [60] T. Zack, T. Claverie, S. Patek, *J. Exp. Biol.* **2009**, *212*, 4002.
- [61] S. Patek, B. Nowroozi, J. Baio, R. Caldwell, A. Summers, *J. Exp. Biol.* **2007**, *210*, 3677.
- [62] G. M. Bond, R. H. Richman, W. P. McNaughton, *J. Mater. Eng. Perform.* **1995**, *4*, 334.
- [63] P. Calvert, *J. Mater. Sci. Eng. C* **1994**, *12*, 69.
- [64] A. Oliveira, J. Mano, R. Reis, *Curr. Opin. Solid State Mater. Sci.* **2003**, *7*, 309.
- [65] L. Addadi, S. Weiner, *Angew. Chem., Int. Ed.* **1992**, *31*, 153.
- [66] J. Aizenberg, G. Lambert, L. Addadi, S. Weiner, *Adv. Mater.* **1996**, *8*, 222.
- [67] L. B. Gower, D. J. Odom, *J. Cryst. Growth* **2000**, *210*, 719.
- [68] S. Weiner, L. Addadi, *J. Mater. Chem.* **1997**, *7*, 689.
- [69] F. E. Coblenz, T. H. Shafer, R. D. Roer, *Comp. Biochem. Physiol., Part B: Biochem. Mol. Biol.* **1998**, *121*, 349.
- [70] N. Tsutsui, K. Ishii, Y. Takagi, T. Wantanabe, H. Nagasawa, *Zool. Sci.* **1999**, *16*, 619.
- [71] L. Addadi, S. Raz, S. Weiner, *Adv. Mater.* **2003**, *15*, 959.
- [72] S. Weiner, Y. Levi-Kalisman, S. Raz, L. Addadi, *Connect. Tissue Res.* **2003**, *44*, 214.
- [73] S. Raz, O. Testeniere, A. Hecker, S. Weiner, G. Luquet, *Biol. Bull.* **2002**, *203*, 269.
- [74] T. Y.-J. Han, J. Aizenberg, *Chem. Mater.* **2008**, *20*, 1064.
- [75] A. L. Goodwin, M. Michel, B. L. Phillips, D. A. Keen, M. T. Dove, R. J. Reeder, *Chem. Mater.* **2010**, *22*, 3197.
- [76] L. B. Gower, *Chem. Rev.* **2008**, *108*, 4551.
- [77] R. S. K. Lam, J. M. Charnock, A. Lennie, F. C. Meldrum, *CrystEngComm* **2007**, *9*, 1226.
- [78] E. Belamie, G. Mosser, F. Gobeaux, M. Giraud-Guille, *J. Phys.: Condens. Matter* **2006**, *18*, S115.
- [79] R. Marchessault, F. Morehead, N. Walter, *Nature* **1959**, *184*, 632.
- [80] L. Onsager, *Ann. N. Y. Acad. Sci.* **1949**, *51*, 627.
- [81] J. Li, J.-F. Revol, E. Naranjo, R. Marchessault, *Int. J. Biol. Macromol.* **1996**, *18*, 177.
- [82] J. Li, J.-F. Revol, R. Marchessault, *J. Colloid Interface Sci.* **1997**, *192*, 447.
- [83] J. Revol, R. Marchessault, *Int. J. Biol. Macromol.* **1993**, *15*, 329.
- [84] J. Li, J.-F. Revol, R. Marchessault, *J. Appl. Polym. Sci.* **1997**, *65*, 373.
- [85] J. Li, J.-F. Revol, R. Marchessault, *J. Colloid Interface Sci.* **1996**, *183*, 365.

- [86] E. Belamie, P. Davidson, M. Giraud-Guille, *J. Phys. Chem. B* **2004**, *108*, 14991.
- [87] D. Gray, *Carbohydr. Polym.* **1994**, *25*, 277.
- [88] X. M. Dong, D. G. Gray, *Langmuir* **1997**, *13*, 3029.
- [89] L. Besseau, M.-M. Giraud-Guille, *J. Mol. Biol.* **1995**, *251*, 197.
- [90] P. Calvert, P. Rieke, *Chem. Mater.* **1996**, *8*, 1715.
- [91] A.-W. Xu, Y. Ma, H. Colfen, *J. Mater. Chem.* **2006**, *17*, 415.
- [92] J. J. D. Yoreo, A. Wierzbicki, P. M. Dove, *CrystEngComm* **2007**, *9*, 1144.
- [93] Y. Bouligand, *Comptes rendus Palevol* **2004**, *3*, 617.
- [94] J. G. Fernandez, D. E. Ingber, *Adv. Mater.* **2012**, *24*, 480.
- [95] K. S. Chow, E. Khor, *Biomacromolecules* **2000**, *1*, 61.
- [96] G. Cardenas, P. Anaya, C. v. Plessing, C. Rojas, J. Sepulveda, *J. Mater. Sci.: Mater. Med.* **2008**, *19*, 2397.
- [97] P. Morganti, G. Morganti, A. Morganti, *Nanotechnol., Sci. Appl.* **2011**, *4*, 123.
- [98] E. Khor, L. Y. Lim, *Biomaterials* **2003**, *24*, 2339.
- [99] M. Miessner, M. G. Peter, J. F. V. Vincent, *Biomacromolecules* **2001**, *2*, 369.
- [100] S. Hirano, *Agric. Biol. Chem.* **1978**, *42*, 1939.
- [101] K. S. Chow, E. Khor, A. C. A. Wan, *J. Polym. Res.* **2001**, *8*, 27.
- [102] A. C. Wan, E. Khor, G. W. Hastings, *J. Biomed. Mater. Res.* **1998**, *41*, 541.
- [103] G. Falini, S. Fermani, *Tissue Eng.* **2004**, *10*, 1.
- [104] C. Muzzarelli, R. A. Muzzarelli, *J. Inorg. Biochem.* **2002**, *92*, 89.
- [105] T. Kato, T. Amamiya, *Chem. Lett.* **1998**, *3*, 199.
- [106] S. Zhang, K. Gonsalves, *J. Appl. Polym. Sci.* **1995**, *56*, 687.
- [107] S. Zhang, K. E. Gonsalves, *Mater. Sci. Eng., C* **1995**, *3*, 117.
- [108] A. Sugawara, T. Kato, *Chem. Commun.* **2000**, 487.
- [109] L. Addadi, S. Weiner, *Proc. Natl. Acad. Sci.* **1985**, *82*, 4110.
- [110] M. Gunthorpe, C. Sikes, A. Wheeler, *Biol. Bull.* **1990**, *179*, 191.
- [111] W. Li, L. Liu, W. Chen, L. Yu, W. Li, H. Yu, *Process Biochem.* **2010**, *45*, 1017.
- [112] L. Gower, D. Tirrell, *J. Cryst. Growth* **1998**, *191*, 153.
- [113] X. Cheng, P. L. Varona, M. J. Olszta, L. B. Gower, *J. Cryst. Growth* **2007**, *307*, 395.
- [114] S. D. Sims, J. M. Didymus, S. Mann, *Chem. Commun.* **1995**, 1031.
- [115] J. Aizenberg, D. A. Muller, J. L. Grazul, D. R. Hamann, *Science* **2003**, *299*, 1205.
- [116] J. M. Didymus, P. Oliver, S. Mann, A. L. DeVries, P. V. Hauschka, P. Westbroek, *J. Chem. Soc., Faraday* **1993**, *89*, 2891.
- [117] J. R. Clarkson, T. J. Price, C. J. Adams, *J. Chem. Soc., Faraday* **1992**, *88*, 243.
- [118] Y. Politi, D. R. Batchelor, P. Zaslansky, B. F. Chmelka, J. C. Weaver, I. Sagi, S. Weiner, L. Addadi, *Chem. Mater.* **2010**, *22*, 161.
- [119] S. O. Anderson, *Comp. Biochem. Physiol., Part A: Mol. Integr. Physiol.* **1999**, *123*, 203.
- [120] M. Nousiainen, K. Rafn, L. Skou, P. Roepstorff, S. O. Anderson, *Comp. Biochem. Physiol.* **1998**, *199*, 189.
- [121] M. Kragh, L. Molbak, S. O. Anderson, *Comp. Biochem. Physiol., Part B: Biochem. Mol. Biol.* **1997**, *118*, 147.
- [122] E. Loste, F. C. Meldrum, *Chem. Commun.* **2001**, 901.
- [123] S. Raz, S. Weiner, L. Addadi, *Adv. Mater.* **2000**, *12*, 38.
- [124] E. Loste, R. M. Wilson, R. Seshadri, F. C. Meldrum, *J. Cryst. Growth* **2003**, *254*, 206.
- [125] D. Wang, A. F. Walalce, J. J. D. Yoreo, P. M. Dove, *Proc. Natl. Acad. Sci.* **2009**, *106*, 21511.
- [126] C. S. Martens, R. C. Harriss, *Geochim. Cosmochim. Acta* **1969**, *34*, 621.
- [127] A. Boskey, A. Posner, *Mater. Res. Bull.* **1974**, *9*, 907.
- [128] J. Tao, D. Zhou, Z. Zhang, X. Xu, R. Tang, *Proc. Natl. Acad. Sci.* **2009**, *106*, 22096.
- [129] S. Raz, P. C. Hamilton, F. H. Wilt, S. Weiner, L. Addadi, *Adv. Funct. Mater.* **2003**, *13*, 480.
- [130] Y. Levi-Kalisman, S. Raz, S. Weiner, L. Addadi, I. Sagi, *J. Chem. Soc., Dalton Trans.* **2000**, 3977.
- [131] C. Gunther, A. Becker, G. Wolf, M. Eppe, *Z. Anorg. Allg. Chem.* **2005**, *631*, 2830.
- [132] G. Wolf, C. Gunther, *J. Therm. Anal. Calorim.* **2001**, *65*, 687.
- [133] M. Faatz, F. Grohn, G. Wegner, *Adv. Mater.* **2004**, *16*, 996.
- [134] F. M. Michel, J. MacDonald, J. Feng, B. L. Phillips, L. Ehm, C. Tarabrella, J. B. Parise, R. J. Reeder, *Chem. Mater.* **2008**, *20*, 4720.
- [135] A. Becker, U. Bismayer, M. Eppe, H. Fabritius, B. Hasse, J. Shi, A. Ziegler, *J. Chem. Soc., Dalton Trans.* **2003**, 551.
- [136] L. Brecevic, A. E. Nielsen, *J. Cryst. Growth* **1989**, *98*, 504.
- [137] A. Radha, T. Z. Forbes, C. E. Killian, P. Gilbert, A. Navrotsky, *Proc. Natl. Acad. Sci.* **2010**, *107*, 16438.
- [138] E. E. Wilson, A. Awonusi, M. D. Morris, D. H. Kohn, M. M. Tecklenburg, L. W. Beck, *Biophys. J.* **2006**, *90*, 3722.
- [139] P. Raiteri, J. D. Gale, *J. Am. Chem. Soc.* **2010**, *132*, 17623.
- [140] J. W. Singer, A. O. Yazaydin, R. J. Kirkpatrick, G. M. Bowers, *Chem. Mater.* **2012**, *24*, 1828.
- [141] K. Naka, Y. Chujo, *Chem. Mater.* **2001**, *13*, 3245.
- [142] C. Li, D. L. Kaplan, *Curr. Opin. Solid State Mater. Sci.* **2003**, *7*, 265.
- [143] B. R. Heywood, S. Mann, *Chem. Mater.* **1994**, *6*, 311.
- [144] S. Mann, B. R. Heywood, S. Rajam, D. Birchall, *Nature* **1988**, *334*, 692.
- [145] E. DiMasi, V. M. Patel, M. Sivakumar, M. J. Olszta, Y. P. Yang, L. B. Gower, *Langmuir* **2002**, *18*, 8902.
- [146] J. Aizenberg, A. J. Black, G. M. Whitesides, *Nature* **1999**, *398*, 495.
- [147] J. Aizenberg, A. J. Black, G. M. Whitesides, *J. Am. Chem. Soc.* **1999**, *121*, 4500.
- [148] A.-W. Xu, W.-F. Dong, M. Antonietti, H. Colfen, *Adv. Funct. Mater.* **2008**, *18*, 1307.
- [149] H. Colfen, M. Antonietti, *Langmuir* **1998**, *14*, 582.
- [150] M. Antonietti, M. Breulmann, C. G. Goltner, H. Colfen, K. K. W. Wong, D. Walsh, S. Mann, *Chem. Eur.* **1998**, *4*, 2493.
- [151] H. Endo, D. Schwahn, H. Colfen, *J. Chem. Phys.* **2004**, *120*, 9410.
- [152] H. Colfen, *Macromol. Rapid Commun.* **2001**, *22*, 219.
- [153] M. Sedlak, M. Antonietti, H. Colfen, *Macromol. Chem. Phys.* **1998**, *199*, 247.
- [154] B. Guillemet, M. Faatz, F. Grohn, G. Wegner, Y. Gnanou, *Langmuir* **2006**, *22*, 1875.
- [155] M. Basko, P. Kubisa, *J. Polym. Sci., Part A: Polym. Chem.* **2003**, *42*, 1189.
- [156] H. D. Espinosa, J. R. Rim, F. Barthelat, M. J. Buehler, *Prog. Mater. Sci.* **2009**, *54*, 1059.
- [157] G. M. Luz, J. F. Mano, *Trans. R. Soc., A* **2009**, *367*, 1587.
- [158] L. C. Palmer, C. J. Newcomb, S. R. Kaltz, E. D. Spörke, S. I. Stupp, *Chem. Rev.* **2008**, *108*, 4754.
- [159] M. Paillet, A. Dufresne, *Macromolecules* **2001**, *34*, 6527.
- [160] Y. Lu, L. Weng, L. Zhang, *Biomacromolecules* **2004**, *5*, 1046.
- [161] K. G. Nair, A. Dufresne, *Biomacromolecules* **2003**, *4*, 657.
- [162] K. G. Nair, A. Dufresne, *Biomacromolecules* **2003**, *4*, 666.
- [163] K. G. Nair, A. Dufresne, *Biomacromolecules* **2003**, *4*, 1835.
- [164] B. Chen, X. Peng, W. Wang, J. Zhang, R. Zhang, *Micron* **2002**, *571*.
- [165] S. L. Gunderson, J. A. Lute, *J. Reinf. Plast. Compos.* **1993**, *12*, 559.
- [166] B. Chen, X. Peng, C. Cai, H. Niu, X. Wu, *Mater. Sci. Eng., A* **2006**, *423*, 237.
- [167] T. Apichatrabrut, K. Ravi-Chandar, *Mech. Adv. Mater. Struct.* **2006**, *13*, 61.
- [168] L. Cheng, A. Thomas, J. L. Glancey, A. M. Karlsson, *Composites: Part A* **2011**, *42*, 211.
- [169] K. Ravi-Chandar, *Army Research Report W911NF-05-1-0065* **2011**, 1–46.

- [170] L. K. Grunenfelder, N. Suksangpanya, C. Salinas, G. Milliron, N. Yaraghi, S. Herrera, K. Evans-Lutterodt, S. R. Nutt, P. Zavattieri, D. Kisailus, *Acta Biomater.* **2014**, DOI: 10.1016/j.actbio.2014.03.022.
- [171] P. Fratzl, H. S. Gupta, F. D. Fisher, O. Kolednik, *Adv. Mater.* **2007**, *19*, 2657.
- [172] K. E. Tanner, *Science* **2012**, *336*, 1237.
- [173] Z. Burghard, L. Zini, V. Srot, P. Bellina, P. A. v. Aken, J. Bill, *Nano-Lett.* **2009**, *9*, 4103.
- [174] P. Murali, T. K. Bhandakkar, W. L. Cheah, M. H. Jhon, H. Gao, R. Ahluwalia, *Phys. Rev. E: Stat., Nonlinear, Soft Matter Phys.* **2011**, *84*, 015102.
- [175] I. Zlotnikov, I. Gotman, Z. Burghard, J. Bill, E. Gutmanas, *Colloids Surf., A* **2010**, *361*, 138.
- [176] A. Tasdemirci, G. Tunusoglu, M. Guden, *Int. J. Impact Eng.* **2012**, *44*, 1.
- [177] A. Bose, *Adv. Powder Metall. Part. Mater.* **1992**, *9*, 57.
- [178] *Cutting Tool Engineering* **1992**, *44*, 10.
- [179] University of Stuttgart, Institute for computational design faculty of architecture and urban planning, <http://icd.uni-stuttgart.de/?tag=researchpavilion2012> (accessed November, 2013).
- [180] G. J. d. A. A. Soler-Illia, C. Sanchez, B. Lebeau, J. Patarin, *Chem. Rev.* **2002**, *102*, 4093.

Received: February 28, 2014
Revised: April 12, 2014
Published online: May 15, 2014